Applications of Transition Metal NMR Spectroscopy in Coordination Chemistry

Dieter Rehder*

It is an intriguing task, to probe a complex compound at the metal centre itself instead of relying on secondary informations obtained from the periphery built up by the coordination sphere. Nonetheless, NMR spectroscopy still anchors in (mostly) routine measurements concerned with ligand nuclei such as ^{1}H, ^{13}C, ^{19}F, and ^{31}P. Only very cautiously, inorganic chemists are moving into the promising area of metal NMR. But what is it really, a chemist, working in the fields of coordination chemistry, organometallic chemistry, bioinorganic chemistry or related disciplines, can get out of a metal-NMR spectrum? We shall try to answer this question by (i) elucidating the interpretive background and (ii) presenting a number of illustrative examples where transition metal NMR is exploited to solve problems which otherwise could not easily be dealt with.

1. Introduction

Dealing with the lack of enthusiasm of many (if not most) of the (coordination) chemists as it comes to non-routine nuclei, several reasons for this self-restriction may be spotted. Among these are the lack of suitable instrumentation, difficulties with the interpretation of NMR parameters obtained for the heavier nuclei, and problems with fast relaxation (excessive line widths), especially so if the NMR probe is a quadrupolar nucleus. In many cases, however, these difficulties are merely an outcome of a traditional view and can easily be neutralized. A broad-band ^{13}C emitter, e.g., which belongs to the standard equipment of practically every laboratory, can also be employed for nuclei such as ^{45}Sc, ^{51}V, ^{55}Mn, ^{59}Co or ^{93}Nb, and others. Quadrupolar nuclei (which are those with a nuclear spin $> ½$) may rise problems because of the effective quadrupole relaxation mechanism. But again, this problem is not a severe one where either the quadrupole moment is rather small (^{51}V, ^{95}Mo) or the local symmetry of the complex fairly high ($\geqq C_{3v}$). Rather sharp resonance lines are obtained (except for nuclei with very large quadrupole moments: $^{177,179}Hf$, ^{181}Ta, $^{185,187}Re$, $^{175,176}Lu$, ^{235}U), if the molecule belongs to a cubic point group or, of course, for the spin-½ nuclei. Among the transition elements, ^{57}Fe, ^{89}Y, ^{103}Rh, $^{107,109}Ag$, $^{111,113}Cd$, ^{169}Tm, ^{171}Yb, ^{183}W, ^{195}Pt, and ^{199}Hg belong to this latter category. Further, the disadvantage of reduced resolution with broad lines is, at least partly, overcome by (i) the large shift ranges for most of the transition metal nuclei, covering several thousand ppm (Fig. 1) and reflecting an extreme sensitivity of the nuclei towards even minor changes in the arrangement of the coordination sphere, and (ii) the availability of an additional parameter, viz. the line width, for the comprehensive investigation of a complex.

Thus, in isotropic media, there is a set of three parameters: (1) the line width, quoted as the width of a resonance signal at half-height, $W_{½}$, (2) the chemical shift δ which is related to the shielding constant σ by $\delta = \sigma_0 - \sigma$ (σ_0 refers to the standard), and (3) the scalar (i.e. nuclear spin-spin) coupling constant J, or its reduced form $K = J(4\pi^2/h\gamma_M\gamma_L)$, where γ_M and γ_L are the magnetogyric ratios of the coupling metal and ligand nuclei. Intermolecular dynamics, scalar relaxation, and chemical shift anisotropy relaxation are additional factors contributing to $W_{½}$ and may dominate relaxation rates for spin-½ nuclei. Under anisotropic conditions (meso-phases and crystalline solids), dipole-dipole interactions and, for quadrupolar nuclei, quadrupole splittings of the first and second order come in, which allow, inter alia, the direct determination of the nuclear quadrupole coupling constant, NQC, as a further valuable NMR parameter.

In this article, the impetus of the four prominent NMR parameters (δ or σ, J, $W_{½}$, and NQC) will be described, and we will be concerned with one of the three problems mentioned above, the interpretation of metal-NMR parameters. Only solution NMR (including meso-phases) will be considered. Among the typical problems, where metal-NMR spectra are of considerable usefulness, are the identification of new and the recognition of known compounds, mechanistic studies, and the solution structure of molecules including the underlying electronic interactions between metal centre and ligand sphere. Illustrative examples have been chosen so as to satisfy one of the two main criteria: (i) comprehensive coverage of the applicability by taking into consideration a wide range of problems with a variety of d-block metals, (ii) new developments with a likely impact in future years. In the past, most of the studies have been carried out on a comparatively small number of nuclei, the nuclear properties of which are collated in Table 1 together with useful additional information.

2. The Shielding Parameter (Chemical Shifts)

2.1. Background

For the practicing chemist, a convenient form to express the overall shielding of a nucleus, σ, is equation (1):

$$\sigma = A - b\,\Sigma(E_i - E_0)^{-1} \cdot [\langle r^{-3}\rangle_p\, P + \langle r^{-3}\rangle_d\, D] \qquad (1)$$

Dieter Rehder: Born 1941 in Hamburg. 1961–1967 studies of chemistry at the Universität Hamburg, graduating with the degree Dipl.-Chem.; Ph. D. (Dr. rer. nat.) 1970. Since 1970 teaching and research position at the Chemistry Department, Universität Hamburg, with an interim teaching appointment at the College of Arts, Science, and Technology in Kingston/Jamaica W.I. 1979 Habilitation; 1984 appointment as a Professor of Chemistry at the Universität Hamburg. Since 1979 head of an independent research group; main research areas: Synthesis, structure, and reactivity of hydrido-, nitrosyl-, and carbonyl complexes of the early transition metals.

* *Correspondence:* Prof. Dr. D. Rehder
Institut für Anorganische und Angewandte Chemie
Universität Hamburg
Martin-Luther-King-Platz 6, D–2000 Hamburg 13
(Bundesrepublik Deutschland)

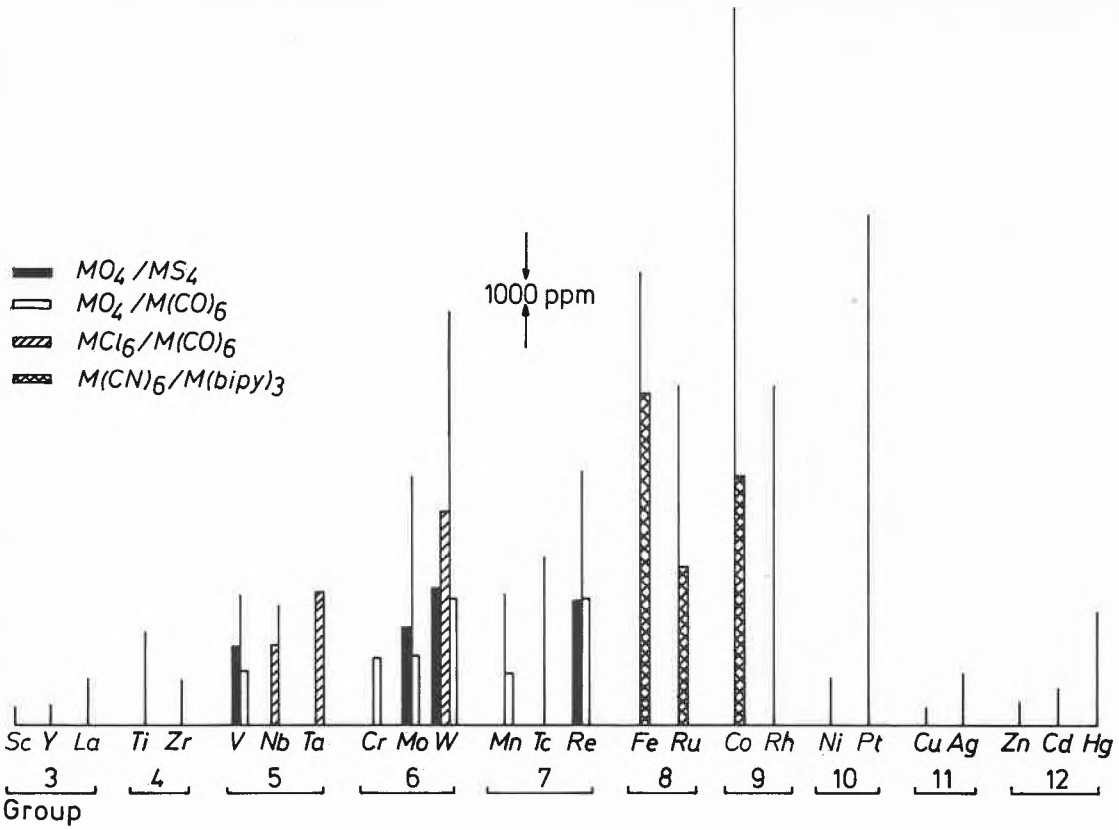

Fig. 1. Overall chemical shift ranges for transition metal compounds in solution, indicated by vertical bars. The length of the bars reflects the present state of knowledge, and the intrinsic NMR sensitivities of the nuclei. A more reliable measure of the relative intrinsic sensitivities arises from the comparison of the shift ranges of pairs of corresponding compounds for different nuclei. This has been indicated by shaded areas for the pairs $\{MO_4\}/\{MS_4\}$ (M = V, Mo, W, Re), $\{MCl_6\}/\{M(CO)_6\}$ (M = Nb, Ta, W), and $\{M(CN)_6\}/\{M(bipy)_3\}$ (M = Fe, Co, Ru) and by open areas for the pair $\{MO_4\}/\{M(CO)_6\}$ (M = V, Cr, Mo, W, Mn, Re) on the basis of data from references [1–7], [8] (Re), and [9] (Ta).

Table 1. Data on transition metal nuclei frequently used in NMR spectroscopy.

Nucleus	Nuclear spin	Quadrupole moment[b]	Receptivity [a] at const. B_0	Receptivity [a] at const. ν_0	ν_0[c]	Shift range[d]	Standard	Reference[e]
^{51}V	7/2	−0.052	0.38	5.52	26.29	3500	$VOCl_3$ neat	[4]
^{55}Mn	5/2	0.33	0.18	2.88	24.66	3500	$[MnO_4]^{\ominus}$/aq.	[3]
^{57}Fe	1/2	–	$3.4\cdot10^{-5}$	0.0032	3.23	12000	Cp_2Fe/solv.	[123]
^{59}Co	7/2	0.42	0.28	4.96	23.61	20000	$[Co(CN)_6]^{3\ominus}$/aq.	[3,123]
^{67}Zn	5/2	0.15	0.0029	0.73	6.25	700	$Zn(ClO_4)_2$/aq.	[3]
^{93}Nb	9/2	−0.2	0.48	8.07	24.44	3300	$[NbCl_6]^{\ominus}$/MeCN	[2b]
^{95}Mo	5/2	−0.02	0.0032	0.76	6.51	6500	$[MoO_4]^{2\ominus}$/aq.	[5]
^{103}Rh	1/2	–	$3.1\cdot10^{-5}$	0.032	3.16	10000	ν(Rh) = 3.16 MHz	[123]
^{113}Cd	1/2	–	0.011	0.22	22.18	1000	$Cd(ClO_4)_2$/aq.	[6]
^{183}W	1/2	–	$7.2\cdot10^{-5}$	0.042	4.16	11000	$[WO_4]^{2\ominus}$/aq.	[5]
^{195}Pt	1/2	–	0.0099	0.22	21.50	14000	$[PtCl_6]^{2\ominus}$/aq.	[7]
^{199}Hg	1/2	–	0.0057	0.18	17.83	3000	$HgMe_2$ neat	[2b]

[a] For an equal number of nuclei per volume unit; relative to ^{1}H = 1 at constant magnetic field B_0 and constant measuring frequency ν_0, respectively. [b] In units of 10^{-28} m^2. For spin-1/2 nuclei, the quadrupole moment, Q, is zero. ^{51}V and ^{95}Mo belong to the low Q category, ^{55}Mn and ^{59}Co to the medium Q category. The high Q category (not contained in this Table) encompasses nuclei with Q values around 2 to 3. [c] Measuring frequency at 2.35 T (^{1}H = 100 MHz). [d] In ppm. [e] The references quoted contain monographs of the individual nuclei; for more general reading see e.g. refs.[1–3].

Non-local contributions (i.e. those by other nuclei present in the molecule) are considered as negligibly small. A and b are constants. A stands for the diamagnetic contribution which, since dominated by the core electrons, is invariable for a given nucleus within the limits of several ppm. This is an important point to state, since NMR spectra of the heavier nuclei (including ^{13}C) are very often mis-interpreted by considering the diamagnetic term in almost the same manner one is used to in ^{1}H-NMR. It has become common, e.g., to relate chemical shift ranges to the oxidation state of the metal. For one thing, this is not necessarily correct (see Fig. 2), and for another thing, doing so (without pointing out the mere phenomenological character of the correlation) implies the – wrong – notion of diamagnetic contributions dominating variations in σ.

The second term in equation (1) is the paramagnetic deshielding contribution, σ(para), which solely is responsible for variations in shielding (and chemical shifts). E_0 and E_i are the energies of the ground state and the excited states, respectively. Only the highest occupied and lowest unoccupied molecular orbitals (HOMO and LUMO, respectively) are of practical importance, and only those E_i contribute which, mediated by the external magnetic field, can mix with the ground state via the angular momentum operator $\hat{L}$ or, in other words, which have the same symmetry properties as $\hat{L}$. This is illustrated in Fig. 3 for a pseudo-octahedral d^6 case under C_{4v} symmetry.

r_p and r_d are the distances of the valence-p and -d electrons from the metal nucleus, and P and D are often termed the «imbalances» of the p and d electrons, leaving it open to the reader to guess what might be meant. As a matter of clarity, we shall replace these terms by the metal LCAO coefficients, C, of the ground and excited state orbitals taking part in transitions. Taking into account that p contributions are small at least in open shell metal complexes (in many cases this is also so in d^0 and d^{10} systems), and introducing a mean energy separation, $\overline{\Delta E}$, we arrive at a simplified but nonetheless extremely useful expression for σ, viz.

$$\sigma = A - b\cdot\overline{\Delta E^{-1}}\langle r^{-3}\rangle_d\,\overline{C_d^2} \qquad (2)$$

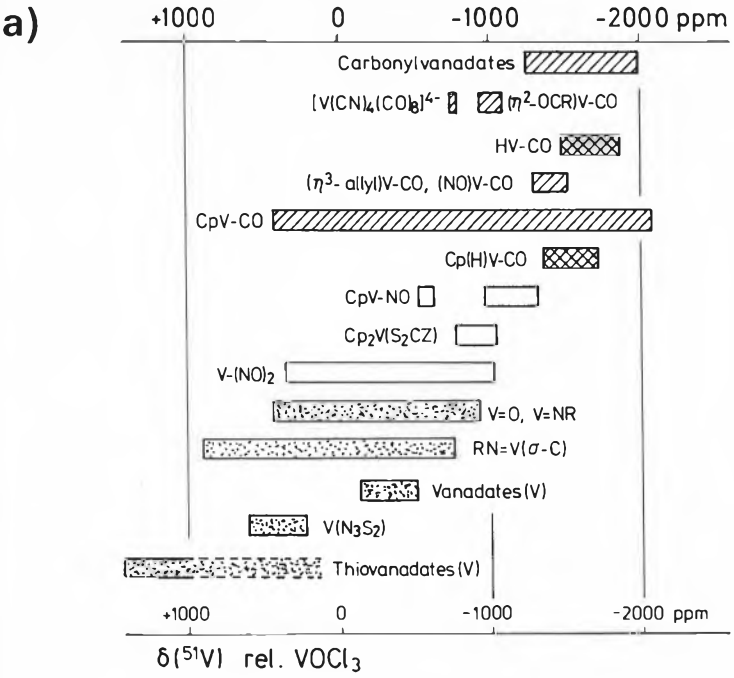

Fig. 2. (a) Shift ranges for vanadium complexes relative to $VOCl_3$, arranged from top to bottom in the order of increasing formal oxidation state (H, η^3-allyl, and NO are considered here as neutral ligands; Cp is η^5-$C_5H_5^{\ominus}$). Punctuated areas: V^{+5}; shaded areas: complexes containing CO ligands, doubly crossed: hydrido complexes; open areas: low-valent, CO-free complexes. This representation demonstrates that the nature of the ligand set is the primary factor responsible for variations in metal shielding. The influence of the oxidation number is a more indirect one: it determines whether a ligand gives rise to a shielding or deshielding contribution. Thus, VOF_3 ($\delta = -632$) is more shielded than $VOBr_3$ (+432), while $[CpV(CO)_3F]^{\ominus}$ (+417) is less shielded than $[CpV(CO)_3Br]^{\ominus}$ (−578). – (b) Expansion for the complexes $[CpV(CO)_3L]$ (V^{+1}), which incorporates the ranges for V^{-1} and most of the V^{+5} compounds. Data are from refs. [3,4], *and from* [10,11] *(derivatives of $[CpV(CO)_4]$),* [12] *(η^2-acyl complexes),* [13] *($[V(NO)_2L_4]^{\oplus}$),* [14] *(V^{+5} containing a V–C σ bond), and* [15] *(cyclothiazeno complexes).*

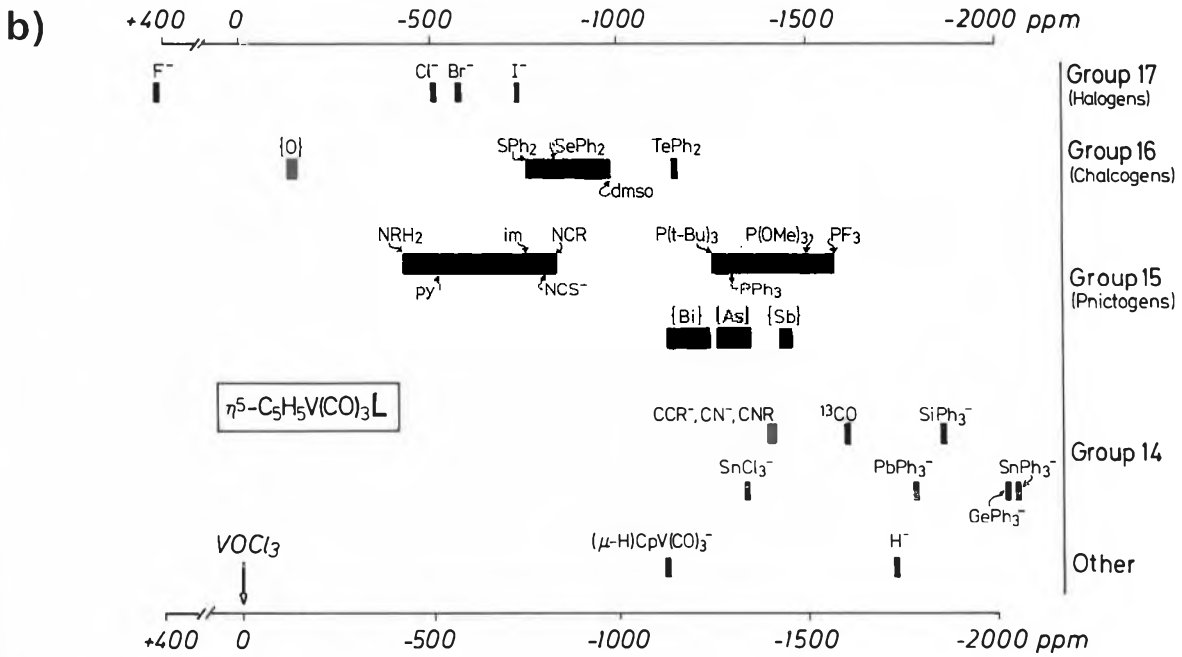

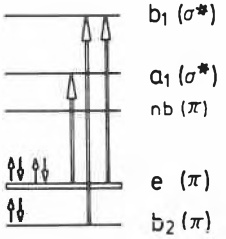

Fig. 3. Schematic presentation of a section of the MO diagram for a $M(d^6)$-complex under local C_{4v} symmetry such as $[V(CO)_5L]^{\ominus}$ or $[Co(CN)_5L]^{3\ominus}$. For strong π interaction, the e and b_2 levels may be interconverted. The $^1A_1$ ground state $[(e)^4(b_2)^2]$ and the three transitions starting from the ground state and contributing to σ(para) are indicated. The corresponding excited states ($^1A_2$ and ^1E) have the same transformation properties as the angular momentum operator $\hat{L}$ ($A_2 + E$). The fourth excited state, $(b_2)^1(e)^4(a_1)^1 = {}^1B_2$, does not contribute. Also, excitations into the non-bonding levels nb(π-CO) do not contribute since their metal-d coefficient tends towards a zero value.*

For complexes of O_h symmetry, the explicit expression is

$$\sigma(O_h) = A - b \cdot [E(T_{2g}) - E(A_{1g})]^{-1} \cdot \langle r^{-3} \rangle_d \, C(T_{2g}) C(A_{1g}) \quad (3)$$

The various simplifications which we have introduced, are justified by the results of calculations of the terms constituting equation (1). A few selected examples are given in Table 2.

2.2. Correlations

If we choose a group of sufficiently similar compounds, we may expect that the factor $\langle r^{-3} \rangle C^2$, in a first approximation, is invariant. In this case, there should be a linear correlation between σ and ΔE or a quantity closely related to ΔE such as a suitable parameter describing the strength of the ligand field, or even an empirical quantity related to the HOMO only. It has been shown, in fact, for the ^{49}Ti-resonances of Cp_2TiX_2 (Cp = η^5-C_5H_5; X = Cl, Br, I), that shielding of the metal nucleus decrea-

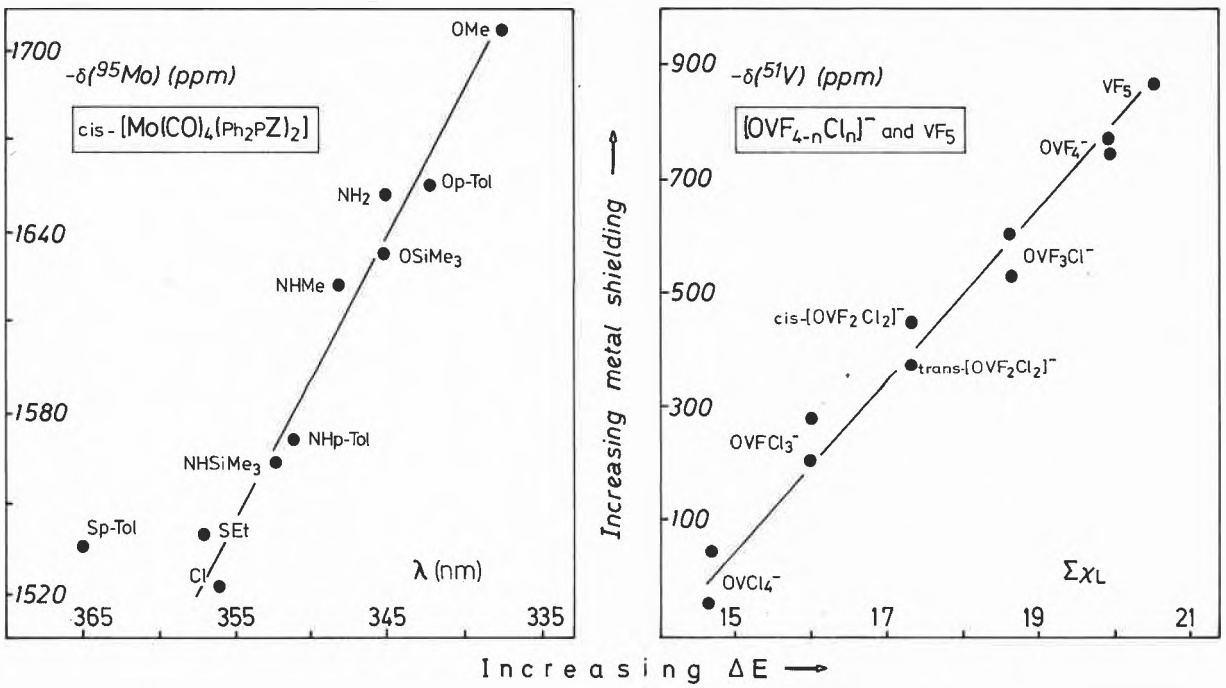

Fig. 4. The correlation of $\delta(^{95}Mo)$ (relative to $[MoO_4]^{2\ominus}$) and $\delta(^{51}V)$ (relative to $VOCl_3$) with ΔE. For the molybdenum complexes [19], ΔE is the lowest UV-VIS absorption; for the vanadium complexes [20], ΔE is represented by the sum of the Allred-Rochow electronegativities χ of all five substituents on V. The differing δ values for some of the complexes are from different sources (cf. ref. [20]). Shielding increases with increasing $\Sigma\chi(L)$ (V-complexes) and $\chi(Z)$ (Mo-complexes). For the series $[Mo(CO)_4(PPh_2Z)_2]$, this relation reflects an increasing π acceptor power of the phosphane ligand.

Table 2. Calculated[a] contributions (in ppm) to the shielding constant for selected complexes of C_{4v} symmetry.

Complex	$\sigma^{\text{non-local}}$	$\sigma_{\text{dia}}^{\text{local}}$[b]	$\sigma_{\text{para}}^{\text{local}}(p)$[c]	$\sigma_{\text{para}}^{\text{local}}(d)$[d]
$[Co(CN)_5OH]^{3\ominus}$	− 0.63	+ 2155.1	− 7.55	− 2331.0
$[Co(NH_3)_5Cl]^{2\oplus}$	− 2.62	+ 2042.9	− 607.1	− 9993.6
$[Mn(CO)_5CN]$	+ 370	+ 1913	− 75	− 13138
$[Mn(CO)_5Cl]$	+ 388	+ 1914	+ 1	− 16276

[a] Calculated on the basis of *Pople*'s model for nuclear shielding in conjunction with INDO parameters (cobalt complexes[16]) and employing an ab initio SCF-MO method (manganese complexes[17]), respectively. [b] Corresponds to the constant «A» in equations (1) and (2). [c] Metal-p contribution to the paramagnetic term. [d] Metal-d contribution to the paramagnetic term.

Scheme 1

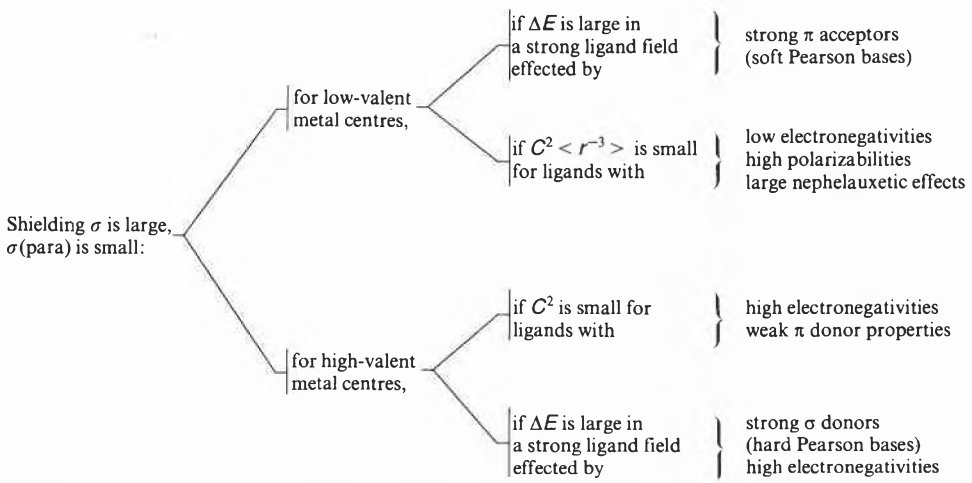

ses with decreasing $Ti(2p_{3/2})$ binding energies[18]. The correlation between σ and a parameter related to ΔE is illustrated by two examples, a series of Mo^0 and V^v complexes, in Fig. 4.

Stated more generally, a strong ligand field increases ΔE and thus increases the overall shielding via a decrease of σ(para). Depending on the nature of the metal centre (its oxidation state) in the coordination compound, a strong ligand can be a strong π acceptor or a strong σ donor (a «hard» base in *Pearson*'s sense, i.e. a ligand with a donor atom exhibiting a high electronegativity and/or low polarizability). The two examples in Fig. 4 represent these two cases. The increase of the shielding with increasing electronegativity χ_L (decreasing polarizability α_L) of halide ligands in the series $[VOCl_{4-n}F_n]^{\ominus}$ is a special case of a very common feature in metal NMR of metals in their highest oxidation (d^0) state, and has been termed «inverse χ_L dependence» of metal shielding[3,21]. It is also observed with group 16 ligands (the most «famous» examples possibly are the $[MoE_4]^{2\ominus}$ ions with E = O, S, Se[22]), and, though less pronounced, with group 14 and 15 ligands and along the periods of the Periodic Table[3].

The «normal» χ_L dependence, i.e. an increase of metal shielding with decreasing χ_L (increasing α_L) is observed, again very commonly, in open shell systems such as $[CpV(CO)_3L]^{\ominus}$ (d^4; cf. Fig. 2b). Clearly, when dealing with complexes of this kind, we can no longer disregard variations of the factor $\langle r^{-3}\rangle$ C^2 in equation (2), a fact which has been recognized for quite some time and more recently summarized and re-interpreted for six-coordinated Co^{III} (d^6) complexes[23,24].

C^2 and $\langle r^{-3}\rangle$ are not as easily quantified as ΔE. Several approaches have been undertaken, among them correlations with the nephelauxetic ratio β_{35}[23-25], electronegativity values and IR-spectroscopic force constants[26], and various substituent constants[12,20,27,28].

Qualitatively, the normal χ_L dependence can be interpreted in terms of variations of

$C^2\langle r^{-3}\rangle$ with the extent of covalency (or ionicity) of the metal-ligand bond: A ligand, which has a comparatively low electronegativity and is easily polarizable ($I^{\ominus}$, $Se^{2\ominus}$, SbR_3, $H^{\ominus}$, σ-bonded alkyls and aryls, $SnR_3^{\ominus}$) give rise to small values of C^2 (note that C relates to the *metal* and attains the value of 1 in the crystal-field approximation) and also to small values of $\langle r^{-3}\rangle$ by displacement of electron density from the metal centre towards the ligand. The three quantities are interrelated with each other. The effects discussed in this section are summarized in Scheme 1. For low-valent complexes, Fig. 2b imparts an illustrative picture.

Electronic effects are not restricted to those directly induced by the coordinating atom of a ligand function but may be mediated through the second or third sphere. In low-valent transition metal complexes, e.g. in carbonyl complexes of the general formula $[M(CO)_n(E{-}Z)]$, where E–Z is a ligand coordinating via E and carrying a substituent Z, a decrease of electron density by electron-withdrawing Z leads to an *in*crease of metal shielding, if there is a π accepting ligand orbital available for strong metal-to-ligand π interaction (see the carbonyl-phosphane-molybdenum complexes in Fig. 4), and to a *de*crease of metal shielding, if this is not so (such as in ring-substituted η^6-arene and η^5-cyclopentadienyl compounds[29,30]).

The electronic situation of a ligand may also be subject to alterations stemming from steric requirements. A bulky ligand, in its effect, is a weak ligand since overlap conditions are unfavourable. As a consequence, ΔE decreases and $C^2\langle r^{-3}\rangle$ increases. These two factors point into the same direction, leading to a decrease of overall shielding. In Fig. 5, steric and electronic effects on ^{51}V shielding are demonstrated for the complexes $[CpV(CO)_3(PZ_3)]$.

Steric effects have also been noted in metallacycles incorporating ^{51}V, ^{93}Nb, ^{59}Co, ^{95}Mo, ^{183}W, and ^{195}Pt (Fig. 6), where the most strained chelate four-membered ring structures give rise to the lowest shielding values. Differing steric conditions are further responsible for the observability of two distinct signals in complexes with two centres of chirality (Fig. 7).

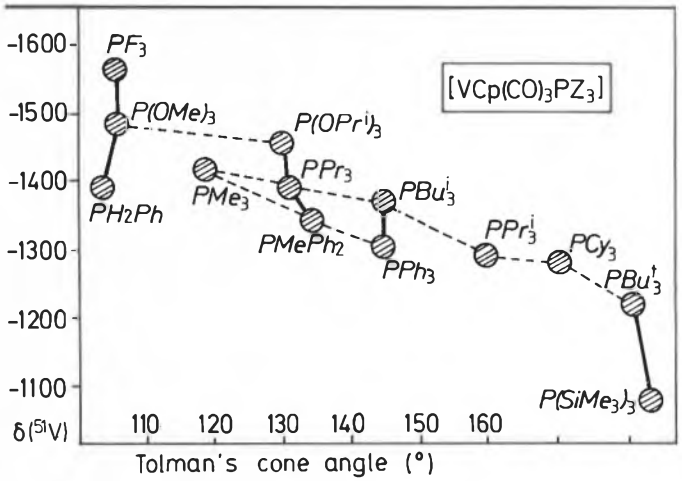

Fig. 5. ^{51}V chemical shifts (relative to $VOCl_3$) of the complexes $[CpV(CO)_3(PZ_3)]$ vs. Tolman's cone angle of the phosphane ligands as a measure of the steric requirement of PZ_3. Dashed lines, sloping from left to right, connect complexes, for which progressive deshielding of the ^{51}V nucleus is primarily affected by increasing steric crowding. Solid lines between complexes containing phosphanes of like cone angle indicate effects primarily electronic in nature. Data from ref. [31].

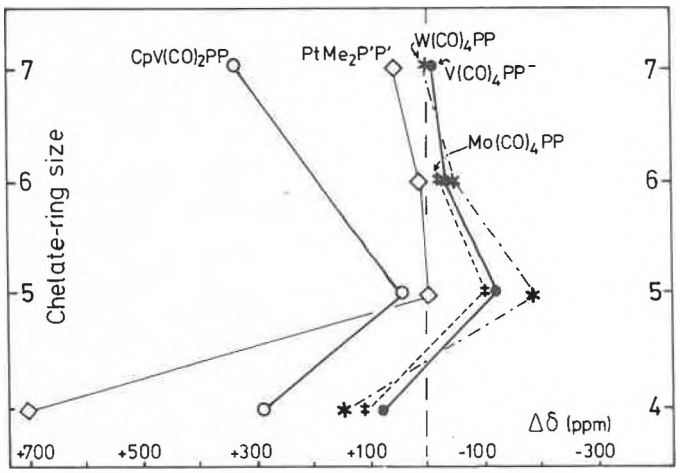

Fig. 6. Dependence of metal shielding in some bis(phosphane) complexes upon the chelate-ring size. Indicated are the shift values $\Delta\delta$ relative to a non-cyclic analogue. A common feature for all five series is the high shielding in five-rings and a minimum shielding in strained four-ring structures. $PP = Ph_2P(CH_2)_nPPh_2$, $P'P' = Me_2P(CH_2)_nPMe_2$. The non-cyclic analogues are complexes containing 2 $PMePh_2$ (V), PMe_2Ph (Mo and W), or PMe_3 (Pt). Data are from refs. [3,31] *(V),* [12] *(Mo, W), and* [33] *(Pt).*

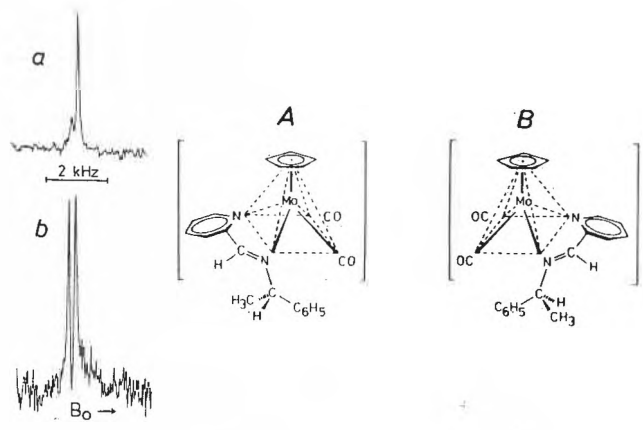

*Fig. 7. 16.3 MHz ^{95}Mo-NMR spectra of mixtures of the diastereomeric Schiff base complexes **A** and **B**, differing only in the molybdenum configuration. The two signals are separated by 14 ppm; the signal at high field corresponds to **A**. The molar ratios are **A**/**B** = 4/1 (a) and 1/1 (b)* [34].

2.3. *Isotope Effect and Temperature Dependence*

The «steric» factor just discussed points to the possibility that changes in nuclear shielding go along with changes in bond lengths and bond angles and hence with molecular parameters which also underly variations with isotopic substitution in the ligand sphere, and with temperature. Here, «isotope effect» and «temperature effect» refer to a defined species which is *not* in equilibrium, of any kind, with other components of the global system. Both effects are intimately related to each other and can be understood, as the rotational and

vibrational fine-structure of the electronic levels participating in electronic excitations (mainly so the HOMO) is taken into account: Decreasing occupation of vibronically excited (ground state) levels with decreasing temperature leads to an increase of ΔE in equation (2) and hence to an increase of σ. An equivalent effect is responsible for the more effective shielding observed for the heavier isotopomers on isotopic substitution. The effects are usually small (0.1 to 5 ppm per isotopic substitution; 0.1 to 1.5 ppm per degree). The extent to which isotope and temperature shifts are observed is also related to the actual shielding values for a given nucleus in different environments, and to the overall shielding range of a nucleus. The latter fact might be exploited to quantify intrinsic shielding sensitivities (cf. Fig. 1). Selected values are given in Table 3, and an illustrative example is displayed in Fig. 8.

A semi-quantitative approach, taking into account the «rovibrational» effects upon internuclear distances, and allowing the calculation of isotope shifts, has been developed by *Jameson* and *Osten* on the basis of an expansion of the shielding in terms of internal displacement coordinates Δr (for the bond displacements) and $\Delta\alpha$ (for angle deformations)[41].

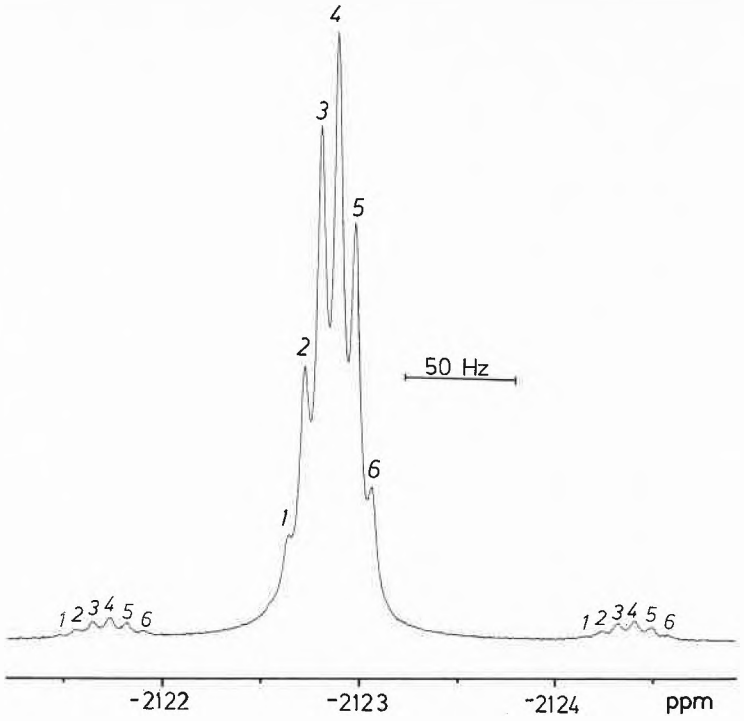

Fig. 8. 88.29 MHz ^{93}Nb-NMR spectrum of $C^{18}O$-enriched $[Nb(CO)_6]^{\ominus}$[40]. The isotopomers $[Nb(C^{16}O)_{6-n}(C^{18}O)_n]^{\ominus}$ are indicated by arabic numerals corresponding to n. Also observable is the doublet for naturally abundant ^{13}CO ($^1J(^{13}C\text{-}^{93}Nb) = 236$ Hz), showing the fine-structure due to $C^{18}O$ isotopomerism. The isotope shifts are −0.085 (^{18}O) and −0.173 ppm (^{13}C) per isotope substitution. The ppm scale is relative to $NbCl_5$ in CH_3CN.

2.4. Intermolecular Exchange

NMR spectroscopy is a millisecond spectroscopy and hence a «slow» method. If there is more than one species present in solution, and if these species are in mutual equilibria with each other, the resonance signal observed at temperatures where the exchange is fast on the NMR time-scale represents a weighted average of the shifts of the various species in equilibrium. The observed chemical shift, δ(obs), can then be expressed by $\delta(\text{obs}) = \Sigma\delta_i x_i$, where δ_i and x_i are the shifts and the mole fractions of the components i[42]. The signal position can vary as a function of the surrounding medium, concentration, temperature, and pH. Several examples will be discussed in the succeeding section. The anomalous isotope effect for zinc halides dissolved in water (a down-field shift of the ^{67}Zn resonance in ^2H_2O relative to ^1H_2O)[43], where several species of the kind $[Zn(H_2O)_{6-n}X_n]X_{2-n}$ are present, likely is a consequence of a more pronounced participation of halide ligands in the first coordination sphere in heavy water. An equilibrium isotope effect has been observed, apart from the static effect (see above), for $[Co(NH_3)_6]Cl_3$ dissolved in $^1H_2O/^2H_2O$[36].

Table 3. Temperature and isotope effects for selected cobalt and vanadium complexes[a].

	Chemical shift[b]	Isotope effect[c]	Temperature gradient[b] (ppm/deg)
^{59}Co[d]			
$[Co(N^{1,2}H_3)_6]^{3\oplus}$	+ 8150	− 5.6	− 1.55[e]
$[Co(^{12,13}CN)_6]^{3\ominus}$		− 0.914	− 1.38
$[Co(C^{14,15}N)_6]^{3\ominus}$		− 0.197	
^{51}V[f]			
$[V(^{16,18}O)_4]^{\ominus}$	− 541	− 0.19	[g]
$[CpV(^{12,13}CO)_4]$	− 1534	− 0.46	− 0.61
$[V(^{12,13}CO)_6]^{\ominus}$	− 1952	− 0.27	− 0.38
$[V(C^{16,18}O)_6]^{\ominus}$		− 0.10	

[a] The data (in ppm) are from the following references: Co[35–37], $[VO_4]^{3\ominus}$[38], V-CO[4,39]. [b] For the lightest isotopomer relative to $[Co(CN)_6]^{3\ominus}$ and $VOCl_3$, respectively. [c] Per isotopic substitution. [d] Overall shift range ca. 20000 ppm. [e] Mean value for the temperature range 348–283 K. [f] Overall shift range ca. 3500 ppm. [g] Not investigated.

2.5. Applications

Intrinsic temperature effects, i.e. those which do not involve two or more species in mutual exchange, are small (cf. Table 3), if the ground state of the molecule under consideration is diamagnetic. This is the normal case, since paramagnetic metal centres are usually NMR-«silent». If, however, there is a spin equilibrium between high-spin and low-spin form, the contact interaction between the unpaired electron and the metal nucleus induces shifts considerably apart from that of the low-spin form. The resulting shift of the complex in the equilibrium state is then expected to be largely dependent upon the temperature. A temperature gradient of 113 ppm/deg has in fact been observed for the $Co^{3\oplus}$ spin-crossover complex **1** shown in Fig. 9[44].

A temperature dependent equilibrium between the dimer **2** (Fig. 9) and its monomeric form has been evidenced by ^{51}V-NMR spectroscopy[45]. At room temperature (293 K, 0.083 M in C_6D_6), monomer and dimer are in sufficiently slow exchange and two signals in the intensity ratio 72:28 arise, separated by 157 ppm. **3a** to **3d** in Fig. 9 demonstrate the versatility of solution structures of cyclothiazenovanadium halides, again as evidenced by ^{51}V-NMR[15].

The pH dependence of ^{51}V and ^{183}W resonances in polyvanadates and -tungstates has largely been employed to describe equilibria between non-protonated and protonated species, and also to indicate the protonation sites. Two problems, the already classical investigation of the protonation equilibria involving decavanadate[46] (**4**), and an actual study on a classical molecule, the «paratungstate A»[47] (**5**) are illustrated in Fig. 10. The esterification of ethanol with vanadate(V) is another example of how solution metal-NMR spectroscopy can help to solve a complex problem: Depending on pH, temperature, and molar ratio of the reactants, three species $[H_2VO_4]^{\ominus}$, $[(EtO)VO_3H]^{\ominus}$, and $[(EtO)_2VO_2]^{\ominus}$ have been detected by distinct ^{51}V-NMR signals[48].

An unequivocal structural characterization of various heteropolytungstates with an $X(Z)W_{11}$ core (X, Z = P, V, Ti, Si, Pb) has been achieved by means of one- and two-dimensional ^{183}W-NMR spectroscopy[49–51] and is a powerful demonstration of the usefulness of metal NMR in describ-

ing even complicated structures. We shall come back to an example in section 3.3. Another example, the structural approach to metallothioneins by ^{113}Cd-NMR, will be discussed in section 6. The application of metal NMR to structural problems encountered with cluster compounds in solution has developed rapidly during the last few years. A number of solution structures solved by direct metal-NMR methods are displayed in Fig. 10 (**6**, the $Mo^{4\oplus}$-aqua ion in acidic solution, the structure of which has been subject to speculations for half a century[52]) and in Fig. 11 for selected carbonyl complexes (**7** to **11**), some of which exhibit fluctional behaviour at ambient temperatures. Apart from the spectral patterns and the structural point of view, for which details are sketched in the legend of Fig. 11, it is worth noting that the metal chemical shifts of the phosphite complexes **8** and **9** do not significantly deviate from those of the corresponding pure carbonyl parent compounds. This is in accord with the π acceptor power of $P(OMe)_3$ coming close to that of CO, and hence for the ΔE term in equation (2) governing the shielding in these complexes.

The chemical shift of a metal resonance, sometimes in conjunction with other NMR parameters such as the scalar coupling constant and the line width, can be a useful tool to determine the bonding mode of an ambidentate ligand. This is especially so, if the two or more functions of the ligand under question differ largely in their polarizabilities and/or ligand strengths. This is the case with the thiocyanato ligand. In open-shell complexes, N-coordination induces a down-field shift with respect to S-coordination and therefore allows for the discrimination between $[Pt(NCS)_2(SMe)_2]$, $[Pt(SCN)(NCS)(SMe)_2]$, and $[Pt(SCN)_2(SMe)_2]$[58]. N-coordination of $NCS^{\ominus}$ has been established by ^{59}Co-NMR in mixed $NCS^{\ominus}/NH_3$ and $NCS^{\ominus}$/ethylenediamine complexes of $Co^{3\oplus}$; $[Co(NH_3)_5(SCN)]^{3\oplus}$ in alkaline medium apparently is an exception[59].

Among the many examples for bond assignments described in the literature, only three more shall be mentioned here. The first example is the molybdenum complex $[Mo_2(CO)_8P(p\text{-tolyl})_3]$ (**12**, cf. Fig. 12). While the ^{95}Mo resonance of the mononuclear $[Mo(CO)_5P(p\text{-tolyl})_3]$ is a doublet centred at −1746 ppm (relative to $[MoO_4]^{2\ominus}$), there is only a single singlet for compound **12**, shifted to *higher* field (−1977 ppm). This is in accord with (i) the η^6-coordination of one of the tolyl substituents to one of the Mo centres and (ii) the equilibration of the two Mo sites by a fluctional process involving the rupture of the Mo−P bond[60]. The second example is a joint ^{1}H- and ^{45}Sc-NMR study on $[Cp_3Sc]$. In toluene solution and at lower temperatures, two ^{45}Sc-NMR signals are observed, which fact is interpreted by partial association of monomeric Cp_3Sc to a Cp-bridged dimer (**13**, Fig. 12)[61]. The third example, a ^{55}Mn-NMR study of the doubly bridged manganese complex **14** (Fig. 12)[62], shows two ^{55}Mn-NMR signals separated by 430 ppm. The low-field signal is broad and corresponds to the manganese site coordinated to phosphorus and selenium. The high-field signal with a triplet structure clearly shows that the second Mn atom is coordinated to two P atoms and hence, that a five-ring structure prevails.

Drastic shift differences can be expected in dynamic systems involving ligand exchange, if the nature of ligands in mutual exchange differ largely. Examples are $[Sc(H_2O)_{6-n}Cl_n]^{(3-n)\oplus}$ [63], $[Co(S_2CR)_{3-n}(S_2CR')_n]$ [64], and $[NbCl_{6-n}Br_n]^{3\ominus}$ [65], which have all been investigated using the metal centre as an NMR probe.

In the latter case, *cis*- and *trans*-isomers (n = 2 and 4) have also been observed. In the *cis*-isomer, the ^{93}Nb nucleus is less shielded than in the *trans*-isomer, and a comparable trend has also been described

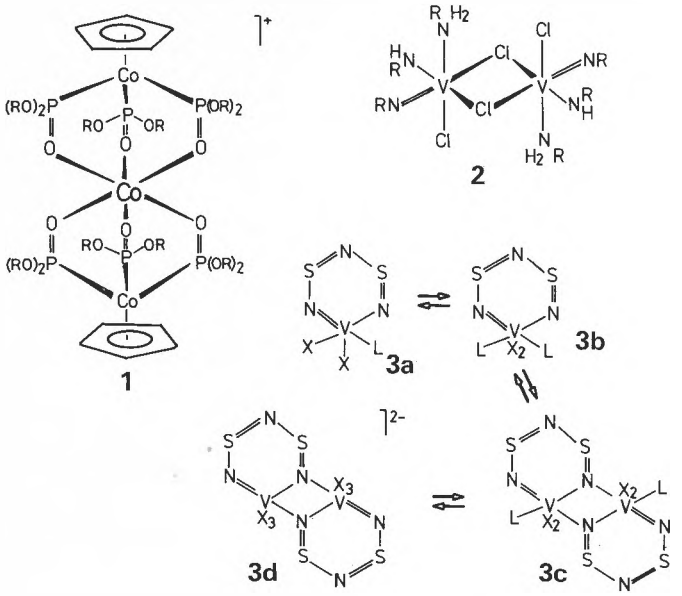

Fig. 9. Solution structures of selected complexes, based on metal-NMR measurements in solution and solid state X-ray structural analyses. **1** *is a spin-cross over* $Co^{3\oplus}$ *complex (central cobalt)* [44] *with a temperature dependent equilibrium between high-spin and low-spin form.* **2** *is in temperature-dependent equilibrium with its monomeric form* $[VCl_2(NtBu)(NHtBu)(NH_2tBu)]$ [45]. *The basic structure of* **3a** *(X = $Cl^{\ominus}$, L = pyridine) is a trigonal bipyramid with L and one of the X in apical positions* [15]. *In the dimeric anion* **3d** *(X = $N_3^{\ominus}$), vanadium is surrounded octahedrally. One of the X and the three N define the tetragonal plane, the two remaining X the axis of the pseudo-octahedron [J. Hanich, M. Krestel, U. Müller, K. Dehnicke, D. Rehder, Z. Naturforsch. B39 (1984) 1686].*

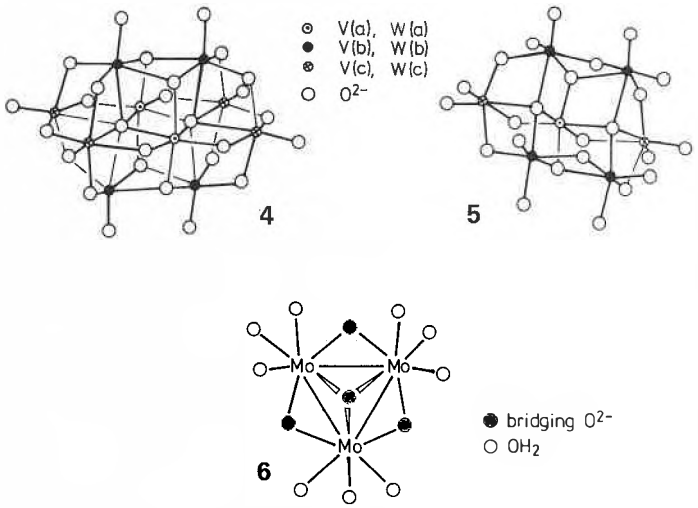

Fig. 10. Idealized structures of $[V_{10}O_{28}]^{6\ominus}$ (**4**), $[W_7O_{24}]^{6\ominus}$ (**5**, *«paratungstate A»*), *and* $[Mo_3O_4(H_2O)_9]^{4\oplus}$ (**6**, *«*$Mo^{4\oplus}\cdot aq$*»*). **4** *shows three signals in the intensity ratio 1/2/2 corresponding to the three vanadium sites a, b, and c in the Keggin structure. The first protonation site for the decavanadate is V(b), the second site is V(c)* [4,46]. *The heptatungstate* **5** *(the seven* WO_6 *polyhedra fall into three structural types a/b/c = 1/4/2) is in pH dependent equilibrium with* $[H_2W_{12}O_{42}]^{10\ominus}$ [47]. *The structure of the molybdenum complex* **6** *is based on the X-ray analysis of* $[Mo_3O_4(methyliminodiacetate)_3]^{2\ominus}$ [52].

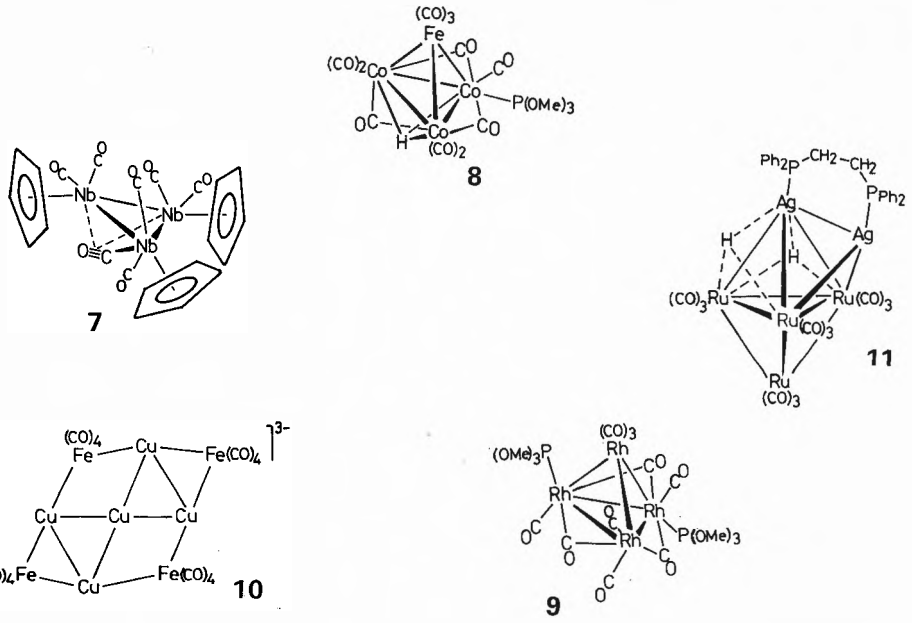

Fig. 11. Solution structures of transition metal carbonyl complexes as established by metal-NMR, partly idealized for clarity and supported by X-ray structures of the crystalline solids. **7**: *$[Cp_3Nb_3(CO)_7]$* [53] *with one of the CO ligands in the η^2-(μ_3-C,μ_2-O) six-electron donating mode. The non-linear temperature dependence of $\delta(^{93}Nb)$ and the half-width of the (single) resonance signal suggests a dynamic component provided by a fluctional process.* **8**: *$[HCo_3Fe(CO)_{11}\{P(OMe)_3\}]$* [54]. *There are two signals in the ^{59}Co-NMR (separated by 64 ppm) in the intensity ratio 1/2, indicating that the phosphite is coordinated to one of the cobalt sites. Another interesting point, which will be dealt with in the forthcoming section (4.), is the broadening of the μ_3-^{1}H and ^{31}P signals by scalar coupling to the ^{59}Co nucleus. In the closely related complex $[HCo_3Fe(CO)_{12}]$, the width of the ^{1}H resonance at half-height at 300 K is 480 Hz!* **9**: *$[Rh_4(CO)_{10}\{P(OMe)_3\}_2]$* [55]. *Four ^{103}Rh resonances at 219 K, spanning an overall range of 253 ppm (the apical Rh is the most shielded one) are indicative of four non-equivalent Rh atoms, i.e. one of the phosphites is in an axial position while the other one occupies a radial site. Only the latter gives rise to a $^2J(^{103}Rh$-$^{31}P)$ splitting (16 Hz) of the Rh signals of the two adjacent, basal Rh atoms. One-bond rhodium-phosphorus coupling in this complex amounts to 209 and 259 Hz.* **10**: *$[Cu_5Fe_4(CO)_{16}]^{3\ominus}$* [56]. *For this complex, one ^{63}Cu resonance for all of the four peripheral Cu atoms is observed which, despite of the fact that ^{63}Cu has a sizable quadrupole moment ($0.16 \cdot 10^{-28}$ m^2), has a width of only 26 Hz, suggesting a high effective symmetry of this cluster by ready interconversion of all of the metal sites.* **11**: *$[H_2Ag_2Ru_4(CO)_{12}$ dppe$]$* [57]. *The cluster has been studied by $^{109}Ag\{^1H\}$-INEPT-NMR, which gives rise to a complicated pattern involving ^{107}Ag-^{109}Ag and ^{109}Ag-^{109}Ag coupling. Only a single silver environment is observed at room temperature, confirming that the cluster undergoes a fluctional process with exchange of the two Ag sites.*

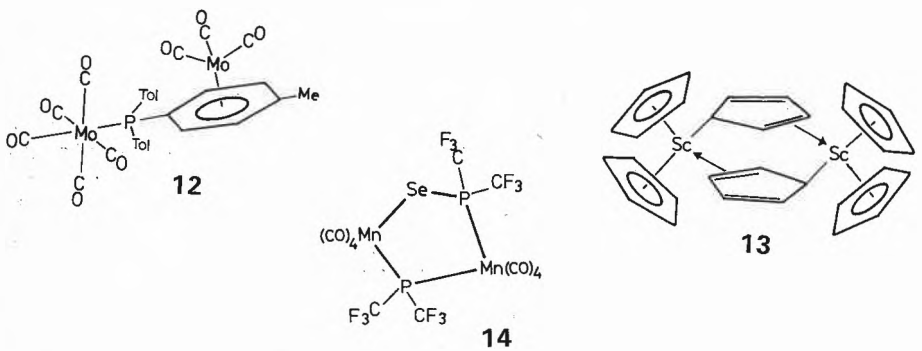

Fig. 12. Assignment of bonding modes for ambidentate ligands. **12:** *Structure of $[Mo_2(CO)_8\{P(p\text{-}Tol)_3\}]$ as established by an X-ray analysis. In solution and at ambient temperatures, the two Mo sites are equilibrated by a fluctional process involving the cleavage of the Mo–P bond* [60]. **13:** *Proposed representation for the dimer $(Cp_3Sc)_2$ formed in nonpolar solvents such as toluene, and in equilibrium with the monomer. The suggested structure is an outcome of a joint ^{1}H- and ^{45}Sc-NMR investigation in the temperature range 303 to 203 K. The bridging Cp ligands are σ and π (η^2-) bonded* [61]. **14:** *The two ^{55}Mn resonance signals at −1283 and −1750 ppm (relative to $[MnO_4]^\ominus$) are typical for the Mn(Se)P and MnP_2 environments, respectively, in an unstrained five-ring structure. In the corresponding four-rings, the signals arrive at −915 for Mn(Se)P in $[\{Mn(CO)_4\}_2(\mu\text{-}SeCF_3)\mu\text{-}P(CF_3)_2]$ and −1353 ppm for MnP_2 in $[\{Mn(CO)_4\}_2\{\mu\text{-}P(CF_3)_2\}_2]$* [62].

for the ^{195}Pt resonances of $[PtCl_{6-n}Br_n]^{2\ominus}$ [66]. One should be careful, however, to extrapolate these findings to other types of complexes; the trends may very well be interconverted. The tendency to generalize trends observed with one specific nucleus in one specific environment, in order to provide a generally applicable, analytical tool, is tempting but dangerous. This does not only apply to the question of isomerism, but also to correlations between metal shifts and oxidation numbers (we have already pointed to this misleading notion), metal shifts and coordination number, or metal shifts and the number of electrons in the coordination sphere. The former has been suggested for linear (AgL_2), trigonal (AgL_3) and tetrahedral (AgL_4) silver complexes [67], the latter for organozirconium complexes with 16 and 18 electrons, respectively [68]. While, in 16-electron species such as [Cp(η^3-allyl)(η^4-butadiene)Zr], the ^{91}Zr nucleus is substantially deshielded, 18-electron complexes, e.g. [Cp_2(η^4-pentadiene)Zr], exhibit shielding values shifted to high field by up to 650 ppm. Although these trends may also be valid for other systems, their general validification awaits a larger variety of material to be studied.

3. Scalar Coupling Constants

3.1. Phenomenology

Electron-mediated (scalar) spin-spin couplings between two nuclei N and N', J(NN'), are commonly observed in well resolved multiplets, if N and N' are spin-½ nuclei. If quadrupolar nuclei are involved, there are two limiting cases:

(1) Coupling is fully effective, giving rise to a multiplet for the nucleus N, say te metal, the structure of which depends upon the number of nuclei N' (the ligand atoms) and the spin of N'. An example is the natural abundant ^{13}C doublet in the ^{93}Nb-NMR spectrum of $[Nb(CO)_6]^\ominus$ [40] shown in Fig. 8. Further examples, the 1/1/1 triplet of the ^{51}V resonances in vanadium amides [20], or the binomial sextet for the ^{51}V resonance of $[V(^{13}CO)_5]^{3\ominus}$ [69] are exhibited in Fig. 13. Spectra of this kind can be expected if the quadrupole moment(s) of N and N' is (are) small (V^{51}, ^{95}Mo, ^{14}N). For nuclei belonging to the medium quadrupole category (quadrupole moment ca. 0.1 to $0.5 \cdot 10^{-28}$ m^2), well resolved spectra are obtained only, if the field gradient at the metal nucleus vanishes, i.e. in complexes of cubic symmetry and in *fac*-[MA_3B_3]. An additional precondition is that the molecular reorientation time, τ, is sufficiently short. τ is a term which will be explained in more detail in the next section. For the time being, we are sufficiently close to the correct meaning of τ, if we interpret it as a factor depending upon the viscosity of the solution. Light, non-polar solvents and small, «spherical» molecules provide low τ values.

(2) The second limiting case, a consequence of *slow* molecular motion and/or

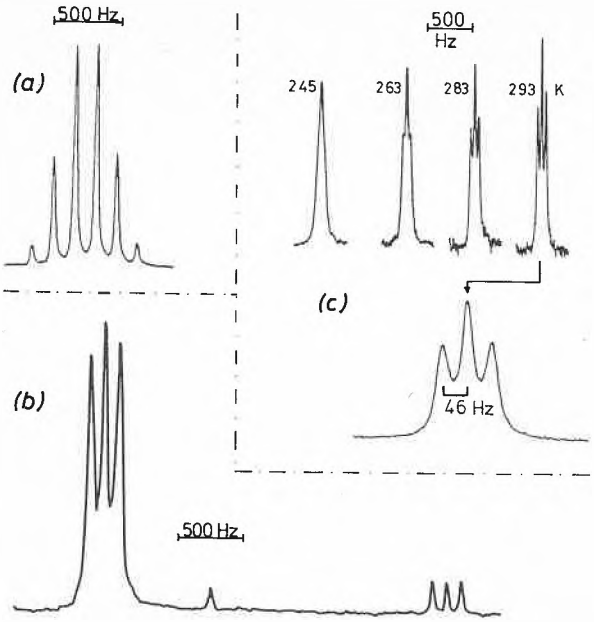

Fig. 13. Three examples for resolved metal-NMR signals exhibiting coupling to ligand nuclei. (a) 77.87 MHz ^{51}V-(quadrupole moment $Q = -0.05$) NMR of $[V(^{13}CO)_5]^{3\ominus}$ ($I(^{13}C) = ½$) [69]. The binomial sextet is the direct proof for the existence of this super-reduced species in ammonia solution. – (b) 23.66 MHz ^{51}V-NMR spectra of $[VO(OR)_2NEt_2]$ (left) and $[VO(OR)_3NEt_2]^{\ominus}$ (right; $I(^{14}N) = 1$, $Q = 0.016$; R is isopropyl), showing the almost ideal 1/1/1 triplet expected for fully effective coupling [20]. The small singlet near the centre is $VO(OR)_3$. – (c) 16.3 MHz ^{95}Mo-($Q = -0.02$) NMR spectra of $[CpMo(NO)(CO)_2]$ in the temperature range 245 to 293 K (the room temperature spectrum is expanded), demonstrating increasing relaxation decoupling as the viscosity of the CH_3CN solution increases with decreasing temperature [70].

large quadrupole moment(s) of N and N′, is the lack of any coupling structure due to complete relaxation decoupling by fast relaxation. The intermediate stages are exemplified in Fig. 13 for the ^{95}Mo resonances of $[CpMo(NO)(CO)_2]$ [70] which, at ambient temperatures, still shows partial coupling to the ^{14}N nucleus of the nitrosyl ligand, and is fully decoupled as the viscosity increases with a drop in temperature.

The coupling information may also be obtained from the NMR spectrum of the ligand atom(s) N′. Again, we have to deal with two limiting cases: (1) If N is a metal belonging to the category of nuclei possessing a low quadrupole moment, or if N is at a highly symmetric site, the signal for N′ usually contains all of the coupling information. Typically, the resonance signal is a resolved, non-binomial multiplet or exhibits a characteristic plateau-like shape, depending on the relative magnitudes of the coupling constant and the line width. Fig. 14 illustrates the two cases for the ^{13}C resonances of the CO groups and the cyclopentadienyl carbons of $[CpNb(CO)_4]$. (2) In complexes of low local symmetry, for metal centres with a medium to high quadrupole moment, and at low temperatures, relaxation decoupling prevails and the signal for N′ is (a sometimes rather sharp) singlet of Lorentzian shape. This may be an advantage for the exact determination of the chemical shift for N′, and it is therefore sometimes useful to scan a spectrum at low temperature to support decoupling. Heteronuclear decoupling by irradiating the frequency of N while probing N′ also effectively improves the spectral resolution. This has recently been demonstrated by ^{17}O $\{^{51}V\}$ and ^{17}O $\{^{93}Nb\}$ experiments on polyvanadates and niobotungstates [71].

The resonances for the nuclei N and N′ are often complementary in the sense that a broad metal resonance (which is indicative of fast quadrupole relaxation) is associated with a sharp resonance for the ligand atom and vice versa.

Heteronuclear coupling constants may amount to several ten thousand hertz such as $^1J(^{195}Pt\text{-}^{117,119}Sn) = 28\,950$ Hz in *cis*-$[PtCl(SnCl_3)(PEt_3)_2]$ [72] or $^2J(^{199}Hg\text{-}^{117,119}Sn) = 41\,480$ Hz in *trans*-$[IrCl(SnCl_3)(HgCl)CO(PR_3)_2]$ [73], but $J(NN')$ which are two to three orders of magnitude smaller are much more common. Apart from couplings through n bonds (^nJ), «through-space» couplings have also been noted sporadically and used as a possible means to detect metal-hydrogen interaction. An example is the 8-formylchinoline complex of $Pt^{2\oplus}$ (**15** in Fig. 15) with $J(^{195}Pt\text{-}^1H) = 13.7$ Hz [74].

3.2. Background Theory and Correlations

It is commonly accepted that coupling constants $J(NN')$ are dominated by the Fermi contact term, viz.

$$J(NN') \propto \gamma_N \gamma_{N'} \Delta E^{-1} |S(0)|^2_N |S(0)|^2_{N'} \sigma(s) \quad (4)$$

γ is the magnetogyric ratio, ΔE the mean triplet excitation energy. The terms $|S(0)|^2$ (the s-electron densities at the nuclei N and N′) and $\sigma(s)$ (the $\sigma(s)$ electron density in the N–N′ bond) are the main factors influencing variations in J for a given pair of N/N′.

Most of the findings to support the validity of equation (4) in the case where metals are involved comes from metal-phosphorus and metal-carbon coupling constants. There are several common features: in a given series of complexes, e.g. $[CpV(CO)_3(PZ_3)]$ [3,75], $[Mo(CO)_5(PZ_3)]$ [76], $[Mn(CNZ)_6]^{\oplus}$ [77] or $[W(CO)_5(CZ_2)]$ [78], an increase of J is observed as

(i) the electronegativity of the substituent Z increases, which fact causes an inductive delocalization of electron density off the ligand nucleus N′ and hence a contraction of the wave function ψ_s (increase of $|S(0)|^2_{N'}$);

(ii) the π acceptor power of the ligand in-

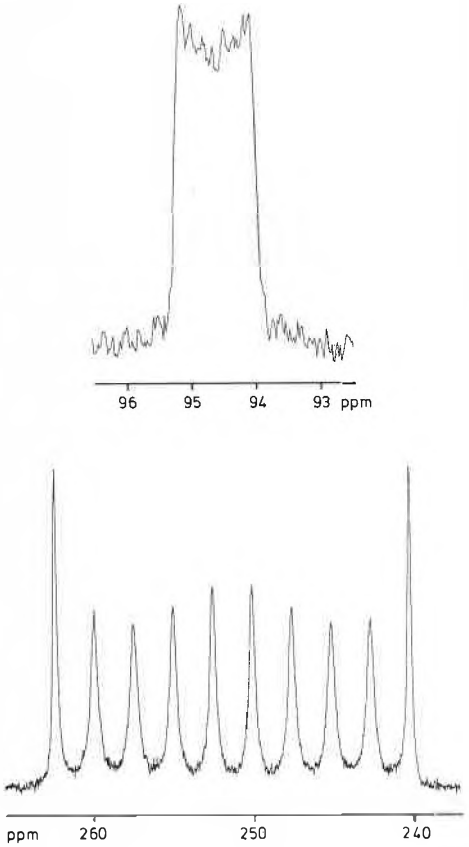

Fig. 14. 90.56 MHz $^{13}C\{^1H\}$-NMR spectrum of $[\eta^5\text{-}C_5H_5Nb(CO)_4]$, 40% ^{13}CO-enriched. (Top) Cp region, (bottom) CO region (scale reduction ¼ relative to the top spectrum). The coupling constants are $^1J(^{93}Nb\text{-}^{13}CO) = 236$ and $J(^{93}Nb\text{-}^{13}C_5H_5) \approx 13$ Hz (estimated from the width of the cyclopentadienyl signal). The ten lines in the carbonyl area are due to the ten possible orientations of the spin-9/2 nucleus ^{93}Nb with respect to the ^{13}C nucleus. The Cp signal is not resolved; however, the characteristic plateau-like shape indicates that coupling is fully effective despite of the comperatively large quadrupole moment of ^{93}Nb ($|Q| = 0.2$) [M. Hoch, D. Rehder, unpublished results].

creases (again as a consequence of increasing electronegativity of Z) diminishing, via metal-to-ligand π delocalization, the electron density at the metal nucleus N and hence increasing $|S(0)|^2_N$;
(iii) the s character of the σ bond between metal and ligand increases with increasing electronegativity of Z. The larger $J(^{183}W\text{-}^{13}C)$ found for carbyne relative to carbene complexes have also been related to a larger $\sigma(s)$ term in the former[79].

A steric effect is also evident: coupling becomes less effective as the bulk of Z and thus of the ligand itself increases.

Further, a dynamic component may come in: The temperature dependence of $^1J(^{199}Hg\text{-}^{31}P)$ in Br_2HgL_2 (L = $PPhBu_2$) dissolved in CH_2Cl_2 (4618 and 4887 Hz at 301 and 165 K, respectively) has been explained by the slowing of the ligand exchange reaction[80]

$$Br_2HgL_2 \rightleftharpoons Br_2HgL + L$$

3.3 Applications

Resolved coupling of a quadrupolar nucleus to a proton is scarcely observed; the coupling constants are usually small and the coupling is swallowed by the overall width of the resonance line. One of the rare examples for resolved coupling is the $^{91}Zr\{^{11}B\}$-NMR spectrum of $[Zr(BH_4)_4]$ (**16**, Fig. 15) which consists of 17 components. Apparently, rapid intramolecular exchange of the hydrogens takes place, imparting an effective T_d environment of the quadrupolar metal nucleus ($Q = -0.21$) and thus minimizing line broadening by quadrupole relaxation[81].

Hydrogen atoms in contact with a quadrupolar metal centre exhibit, in the ^1H-NMR spectrum, broad lines, as long as relaxation decoupling is not yet effective (broad lines may also occur by chemical shift anisotropy relaxation if the metal centre is a spin-½ nucleus; section 4). Quadrupole broadening of the ^1H resonance occurs for the three-centre bridging hydrogen of the cluster **8** in Fig. 11. In tris(1,2-diaminopropane)cobalt$^{3\oplus}$ (**17** in Fig. 15), only the equatorial proton indicated by an asterisk is strongly coupled to the cobalt due to its *trans*-position with respect to the Co–N bond, and therefore gives rise to a broad ^1H resonance[82].

A through-space contact is responsible for the splitting of the ^1H resonance of the formyl proton in the platinum compound **15** (Fig. 15). On the basis of a study of the coupling patterns in the ^{13}C-NMR spectra of ^{57}Fe-enriched α-ferrocenyl carbocations (such as **18** in Fig. 15), σ bonding of the iron atom to the exocyclic carbon atom can be excluded. Rather, the size of the coupling constant is in favour of a fulvenoid π (η^6-) bonding of the ligand. The ^1H-NMR investigation of $[\{Cp_2Y(\mu_2\text{-}H)\}_3(\mu_3\text{-}H)]^{\oplus}$ (**14** in Fig. 15) gave coupling patterns arising from couplings between μ_2-H and μ_3-H, and between the bridging hydrido ligands and the spin-½ nucleus ^{89}Y, indicative of fixed positions of the two types of $H^{\ominus}$[83b].

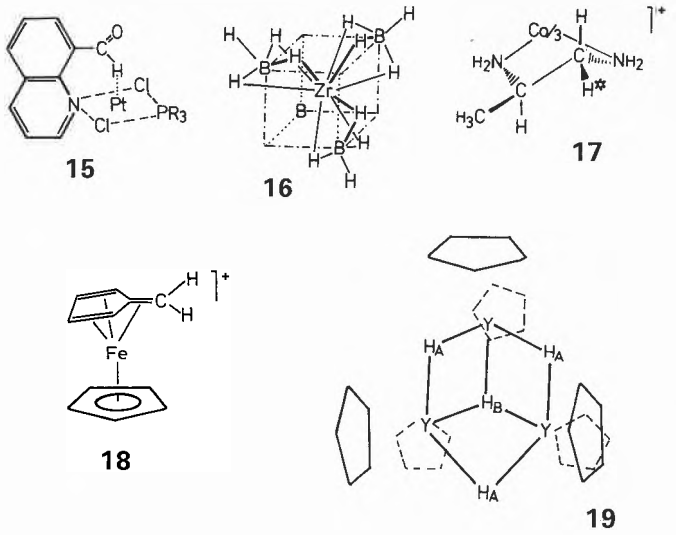

Fig. 15. Metal-hydrogen interactions in selected complexes. **15:** *The $^{195}Pt\text{-}^1H$ coupling constant (13.7 Hz) between the platinum centre of this complex and the hydrogen atom of the formyl group is too large for a five-bond coupling and should therefore indicate direct metal-hydrogen interaction, facilitated by the steric arrangement of the chinoline ligand perpendicular to the plane defined by the $PtCl_2N(P)$ moiety. The Pt–H distance is 230 pm. The data have been obtained from the ^{195}Pt satellites of the ^1H resonance. The satellites are substantially broadened due to chemical shift anisotropy relaxation (section 4) mediated by ^{195}Pt*[74]. **16:** *The $^{91}Zr\{^{11}B\}$-NMR spectrum of this tetrahedral complex exhibits 17 components due to the coupling of Zr to 16 equivalent hydrogens, and thus indicates that terminal and bridging H are in rapid exchange*[81]. *The hydrogen atoms of the fourth boranate ligand have been omitted for clarity.* **17:** *Section of the complex $[Co(1,2\text{-diaminopropane})_3]^{3\oplus}$. The ^1H resonance of the equatorial methylene proton, H*, is broadened due to scalar coupling with $Co^{3\oplus}$. In $[Co(CN)_4(1,2\text{-diaminopropane})]^{\ominus}$, relaxation decoupling occurs because of the lower overall symmetry, resulting in the expected four-line pattern for H**[82]. **18:** *The coupling constant $J(^{57}Fe\text{-}^{13}C)$ in this ferrocenyl cation is ca. 1.5 Hz, which is considerably less than anticipated for a Fe–C σ bond (around 9 Hz), but compares favourably to J(Fe-C) in complexes containing π bonded ligands (1.5 to 4.5 Hz). The J(Fe-C) to the ring carbons are between 2.5 and 4.4 Hz*[83a]. **19:** *The ^1H-NMR of this trinuclear, hydrido-bridged yttrium complex consists of a ten-line multiplet (μ_3-H) and a more complex multiplet for the μ_2-H. The ten-line pattern is the AB part of an AA'A"BYY'Y" spin system with $J(AB) \simeq \frac{1}{2} J(BY)$*[83b]. *More recently, a ^{89}Y-NMR study of* **19** *and related compounds has also appeared*[83c].

The careful assignment of ^{183}W resonances in polytungstates carried out by an analysis of the coupling phenomena has eliminated many inconsistencies in this area and established a firm picture of the solution structure of many of these cluster compounds. An example is $[TiW_{11}PO_{40}]^{5\ominus}$, for which the six ^{183}W resonances have been assigned to six inequivalent tungsten sites by deducing the connectivities between W atoms from two-bond W-O-W couplings[84] (Fig. 16). Homonuclear coupling has also elucidated the structure of cadmium-thionein and will be discussed in the context of applications in bioinorganic chemistry (section 6). A further interesting example for homonuclear coupling has been noted for the $^{199}Hg\text{-}^{199}Hg\text{-}Hg$ and $^{199}Hg\text{-}^{199}Hg\text{-}^{199}Hg$ isotopomers of the linear $[Hg_3]^{2\oplus}$ ion[85] (the natural abundance of the mercury isotope ^{199}Hg is 16.84%). The extremely large coupling constant of 139 600 Hz is brought about by the 6s character of the valence orbitals forming the mercury-mercury bond and the large s electron density at the Hg nucleus (cf. equation (4)) due to relativistic effects for this heavy atom.

Two additional cases for the application of (heteronuclear) coupling phenomena to constitutional problems shall briefly be commented on: Reduction of hexacarbonylvanadate(-I) in liquid ammonia leads to the formation of the «super-reduced» species $[V(CO)_5]^{3\ominus}$. Direct evidence for the existence of this anion with the coordination number 5 for vanadium has been obtained from the binomial sextet of the ^{51}V resonance of $[V(^{13}CO)_5]^{3\ominus}$[69] (see also Fig. 13 (a)). Further, the monohydride $[V(H)(CO)_5]^{2\ominus}$ has been detected through both the ^{51}V- (doublet) and ^1H-NMR (eight-line multiplet[86]; the nuclear spin of ^{51}V is 7/2). Similarly, defined coordination compounds of the constitution $[ScCl_{6-n}\{OP(OEt)_3\}_n]^{(3-n)\ominus}$ (n = 3, 4, or 6) have been identified via the $^2J(^{45}Sc\text{-}^{31}P)$ splittings of the ^{45}Sc-NMR signals[87].

4. Relaxation

The width of a resonance line, usually measured at half-height and quoted as $W_{1/2}$,

is mainly determined by the transversal (spin-spin) relaxation time T_2 which, in non-viscous liquid media, commonly (but not necessarily) is about the same order as the longitudinal (spin-lattice) relaxation time T_1. The choice of the pulse sequence for a specific nucleus is largely dependent on T_1; the knowledge of T_1 values is therefore a necessary precondition to optimize NMR detection especially for nuclei with long T_1 such as ^{57}Fe, ^{103}Rh, or $^{107/109}$Ag[122,123]. T_1 values of spin-½ nuclei are usually governed by chemical shift anisotropy and hence decrease with increasing strength of the applied magnetic field, accompanied with an improvement in detectability of the nucleus[91]. T_2 and $W_{½}$ are connected by the simple relation $W_{½} = (\pi T_2)^{-1}$. Excluding dynamic effects arising from intermolecular exchange processes, there are three major relaxation mechanisms which may considerably shorten T_2 and hence broaden resonance lines.

For quadrupolar nuclei (nuclear spin $I > ½$), the dominating contribution to line broadening comes from quadrupole relaxation (vide infra). For spin-½ nuclei, scalar relaxation, mediated by coupling to a quadrupolar ligand nucleus (such as ^{14}N), can be a main factor, but in low-symmetry complexes, chemical shift anisotropy (CAS) comes in, and this is especially so, if the overall shift range is very large (^{57}Fe, ^{195}Pt). CAS has also been noted for various pseudo-octahedral $Co^{3\oplus}$ complexes as a field-dependent component to the quadrupole-dominated relaxation[88] ($I(^{59}Co) = 7/2$). It is evident that, since the extent of CAS depends upon the magnitude of the applied magnetic field, it is not always desirable to record an NMR spectrum on a high-field instrument.

Severe line broadening due to CAS has been observed in $Pt^{2\oplus}$ complexes both for the ^{195}Pt resonance itself and for the ^{195}Pt satellites in ^{1}H- or ^{13}C-NMR spectra[89,90]. For $[Pt(acac)_2]$, the shielding anisotropy at 4.7 T amounts to about 10000 ppm[89]. In a simplified manner

$$T_2^{-1} \propto B_0^2(\Delta\sigma)^2 f(\tau) \quad (5)$$

where B_0 is the external magnetic field, $\Delta\sigma$ the chemical shift anisotropy ($|\sigma_\parallel - \sigma_\perp|$), and $f(\tau)$ a function of the molecular reorientation time. The presence of this latter term shows that size and bulkiness of the molecule containing the NMR probe are also an important factor to account for, and this has been demonstrated for the ^{57}Fe-NMR spectra of (^{57}Fe-enriched) carbonmonoxide-myoglobin, which gives rise to $W_{½}$ values of 55 Hz (at 8.45 T[91]) and 100 Hz (at 11.7 T[92]) as compared to 2.5 Hz for the slim ferrocene. Scalar contributions arising from ^{57}Fe-^{14}N coupling can be neglected in these compounds.

If the NMR probe is a quadrupole nucleus, four variables determine the size of T_2, viz. a function of the nuclear spin, f(I), the nuclear quadrupole coupling constant NQC, the asymmetry parameter η, and the molecular correlation (or reorientation) time τ. These quantities are linked together by equation (6):

$$T_2^{-1} \; (\simeq T_1^{-1}) \propto f(I) \cdot (NQC)^2 \, (1 + \eta^2/3)\, \tau \quad (6)$$

In non-cubic environments and under isotropic conditions, T_2 and T_1 scarcely deviate largely from each other. In a 1-molal aqueous solution of $ZnSO_4$, e.g., the respective values are 9.3(4) and 9.8(8) ms[93]. NQC is a measure for the interaction («coupling») between the nuclear quadrupole moment Q and the [zz component of the] molecular field gradient [tensor], $\boldsymbol{q}$, at the nucleus. Since Q and f(I) are given quantities for a given nucleus, T_2 becomes directly linked to $\boldsymbol{q}$ and τ (and η, which is zero in axially symmetric complexes and shall not be considered here). Thus, $W_{½}$ is doubled when the above mentioned zinc sulfate solution is 11-mmolal in sodium citrate[93], and this is due to an increase of τ and $\boldsymbol{q}$: As H_2O molecules from the $[Zn(H_2O)_6]^{2\oplus}$ sphere are partially replaced by citrate, the local symmetry is lowered and the complex becomes more bulky and moves less easily through the aqueous medium.

In order to get still closer to the meaning of the two parameters $\boldsymbol{q}$ and τ, let us distinguish between two separate cases: Case (1) is a series of complexes of like local symmetry and almost identical electronic behaviour of the ligand system, such as the complexes $[CpV(CO)_3(PR_3)]$ introduced quite at the beginning of this article (Fig. 5). Varying R from CH_3 to $C(CH_3)_3$ leads to a decrease in T_2 (increase of $W_{½}$) mainly as a result of increasing τ, i.e. slower motion of the molecule. A comparable effect can be achieved by exchanging a non-polar for a polar solvent (hexane → tetrahydrofuran), with more concentrated solutions, or with lower temperatures.

Case (2) is a series of complexes, say $[CpV(CO)_3L]$, where again the local symmetry for all of the species is the same. The ligands L are now chosen so as to minimize steric variations but constituting substantial variations of their electronic nature (e.g. L = CO, CNR, NCR, PH_3, OEt_2, $F^\ominus$). Then, variations of T_2 will mainly be induced by variations in $\boldsymbol{q}$. Unfortunately, these influences are less easily predictable, although, generally, for low-valent metal complexes, resonance lines are sharper if the ligand is a good to excellent π acceptor and/or easily polarizable.

In complexes of cubic symmetry, the field gradient vanishes and with it vanishes the interaction with Q. A very narrow resonance line should result and has in fact been observed with nuclei belonging to the low to medium quadrupole category (cf. the spectrum in Fig. 8). But even in complexes belonging to the cubic point groups, there is usually a residual interaction (and hence a permanent NQC) due to small deviations from the ideal cubic symmetry caused by, inter alia, solvation phenomena, contact-ion pair formation, or the formation of collision complexes. This has been observed for the ^{95}Mo and ^{97}Mo resonances of $[Mo(CO)_6]$ and $[MoE_4]^{2\ominus}$ (E = O, S)[94]. For the hexacarbonyl complex, T_2 values are 340 ms (^{95}Mo) and 45 ms (^{97}Mo). If the nucleus belongs to the high quadrupole category (Q around 2 to $3 \cdot 10^{-28}$ m^2), even minor deviations from O_h or T_d symmetry lead to very short T_2 of ca. 0.1 ms and broad lines of several kHz. Examples are $[TaL_6]^\ominus$ (L = CO, Cl)[9] and $[ReE_4]^\ominus$[8].

5. Quadrupole Interaction in Meso-phases

Under isotropic conditions, the field gradient is modulated by the Brownian motion of the solute molecules and for this reason, quadrupole interactions are confined to a broadening of the NMR line of the quadrupolar metal nucleus. This is not so in mesophases (liquid crystal solutions). These systems are anisotropic to a certain extent, the solute molecules partially aligned in the liquid crystal lattice, and this leads to a splitting of the resonance line into 2I components[95] (Fig. 17). The extent

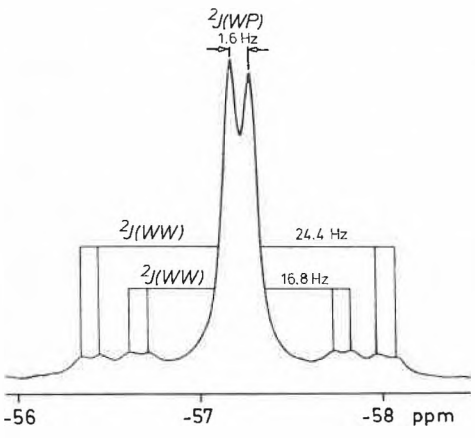

Fig. 16. ^{183}W-NMR signal of one of the six tungsten sites in $[TiW_{11}PO_{40}]^{5\ominus}$. The signal is split into a doublet (1.6 Hz) by $^2J(^{183}W$-$^{31}P)$ coupling; the structure at the base is brought about by two-bond coupling of two different pairwise isotopomers. The natural abundance of ^{183}W is 14.4% [84].

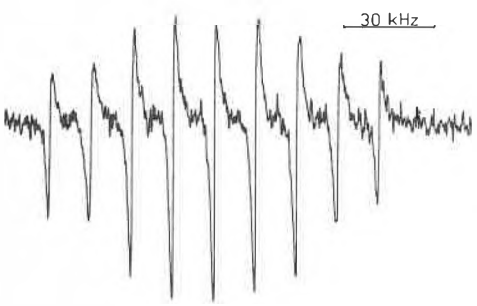

Fig. 17. ^{93}Nb-NMR spectrum (first derivative, obtained on a wide-line instrument at constant measuring frequency) of $[\eta^5$-$C_5H_5Nb(CO)_4]$ dissolved in the nematic liquid crystal Nematic Phase 4 (Merck). The spectrum shows a nine-line pattern characteristic of first order quadrupole splitting for a spin-7/2 nucleus in a partially ordered environment. The ordering factor is 0.30 [97].

of the splitting, $\Delta\nu$, is given by

$$\Delta\nu \propto f(I)\,(NQC)\,S_a \qquad (7)$$

S_a measures the degree of anisotropy and is called the ordering factor. It is hence possible to determine either S_a or NQC from NMR spectra of quadrupolar nuclei in mesophases, if the complementary quantity can be obtained from another experiment.

In this context, and with the next section in mind, we shall draw our attention to an example which possibly suits as a modeling system for the behaviour of an inorganic compound of biological impetus in biomembranes. One of the well established functions of inorganic vanadate is that of an inhibitor of the enzyme ATPase which, inter alia, controls the passage of $Na^{\oplus}$, $K^{\oplus}$, and $Ca^{2\oplus}$ through cellular membranes. In a mixed lyotropic meso-phase (considered here a mimick of the biomembrane) prepared from potassium dodecanate and tetradecylammonium bromide. and treated with vanadate, there are two vanadium species present (assigned $[VO_4H]^{2\ominus}$ and, tentatively, V_4O_{10}) which show quadrupole splitting of the ^{51}V resonance. One of these species ($[VO_4H]^{2\ominus}$) interacts strongly with the carboxylate *and* the alkylammonium ion, the other (V_4O_{10}) with the carboxylate head group only.[96].

6. Applications in Bioinorganic Chemistry

With one exception (^{113}Cd; see below), metal-NMR spectroscopy has not yet extensively been employed to investigate biological systems containing transition metal ions as active (or deactivating) centres. The last few years have shown, however, that this research area is a promising field which is likely to develop rapidly in the near future.

There have been sporadic reports on the detection of bonding interactions between inorganics and bio-molecules by chemical shift and line width variations of the metal-NMR signal. Among these are the binding of oxo- and thiomolybdate to bovine serum albumine[98], the complexes formed between vanadate and uridine or ribonuclease A[99], and the adduct of *cis*-$[Pt(NH_3)_2Cl_2]$ and adenosine monophosphate[100]. The latter example is of special interest for the research work carried out to decode the mode of action of antitumor agents based on $Pt^{2\oplus}$.

A considerable amount of NMR investigations has been done with the nucleus ^{95}Mo in compounds with a possible model character for molybdenum containing enzymes[101-106]. Examples are complexes containing the MoO, *cis*-MoOS, or *cis*-MoO_2 group such as **20** to **22** in Fig. 18. The mono-oxo and di-oxo molybdenum cores are belived to constitute the active sites of the enzymes xanthidine oxidase, sulfite oxidase, and nitrate reductase, and they are also likely an integral part of the iron-molybdenum coenzyme of nitrogenase. Copper-thiomolybdates, e.g. the cluster **23** in Fig. 18, have been investigated in order to establish a ^{95}Mo chemical shift scale, allowing for the distinction of species derived from Cu-Mo interaction. This may have an implication for the biological antagonism between Cu and Mo that leads to copper deficiency in ruminant animals feeding on molybdenum-rich grounds[107,108].

Despite of the successful investigations into these model compounds, it seems doubtful whether, looking actually into the «heart» of a metalloprotein, even a medium level of information will be accessible: In systems, where relaxation is governed by the quadrupole mechanism, the long correlation times τ (equation (6)) for the large protein molecule will broaden the resonance lines to an extent where, if detectable at all, any detailed information gets lost. Thus, the ^{95}Mo resonance of nitrogenase spans a frequency range of about 4.5 MHz[109]!

On the other hand, it has been shown by analyzing changes of line widths, that $Zn^{2\oplus}$ binding to thermolysin, a peptidase isolated from a thermophilic bacterium, is enhanced by addidition of $Ca^{2\oplus}$[110]. Both divalent ions are known to be cooperatively indispensible for the thermostability of the enzyme. Similarly, ^{67}Zn-NMR has been employed, in conjunction with ^{43}Ca-NMR, to study metal-enzyme binding in concanavalin A[111] and calmodulin[112]. Finally, the incorporation of $Zn^{2\oplus}$ in the process of activation of insuline by the formation of hexamers from the insuline unit has again been documented by the broadening of the ^{67}Zn resonance[113]. However, in all these studies, free $Zn^{2\oplus}$ was employed in large excess of the apoprotein. In such a system, the signal observed corresponds to the position of an equilibrium of the kind

$$[Zn(aq)]^{2\oplus} + \text{apoprotein} \rightleftarrows [Zn(\text{protein})]^{2\oplus} + aq$$

with only minor contributions from the zinc-protein to the overall line width, otherwise dominated by the aquazinc cation and, possibly, the exchange process.

The problem of short relaxation times is less stringent if the NMR probe is a spin-½ nucleus, although, as has been extemporated in section 4, slow molecular reorientation and chemical shift anisotropy may also deteriorate spectral resolution (equation (5)). Promising in this respect are ^{57}Fe-NMR studies on «artificial» low-spin $Fe^{2\oplus}$-porphyrins such as iron-*meso*-tetraphenylporphine[114] and their biotic analogues, especially so carbonmonoxide-myoglobin[91,92] mentioned earlier in this article (section 4).

A nucleus which already has attained its merits as an excellent NMR probe into bio-systems is ^{113}Cd. From the increasingly abundant findings, partially reviewed recently[6], we shall pick out the case of cadmium-thionein. Thioneins are small (on the biochemical scale) molecules $M_r \approx 6000$, which serve as a storage and regulatory protein for $Zn^{2\oplus}$ and also as a (temporary) detoxification agent for metal ions such as $Hg^{2\oplus}$ and $Cd^{2\oplus}$. Seven divalent metal ions can be taken up per molecule of apothionein, and the main portion of nowadays knowledge on the metal binding sites comes from ^{113}Cd-NMR analyses[115,116]. The ^{113}Cd-NMR spectra of cadmium-thionein show seven structured resonances in the low-field chemical shift range typical of $Cd^{2\oplus}$ in a tetrahedral environment exclusively built up by thio-ligands (i.e. cystein residues). The seven resonances can be allocated to seven distinct Cd sites divided between a 4-Cd and a 3-Cd sulfur cluster (Fig. 19). The unambiguous site assignments have been carried out on the basis of two-bond and four-bond ^{113}Cd-^{113}Cd connectivities as established by the multiplet splitting of the seven peaks.

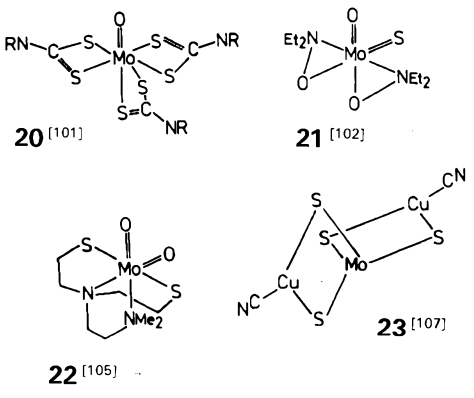

Fig. 18. **20** *to* **22**: *Model compounds for molybdenum containing enzymes.* **23**: *Possible species involved in the molybdenum/copper antagonism. References are given in square brackets.*

7. Applications in Catalysis

Metal-NMR investigations directed towards catalytically active complexes in systems where catalysis actually takes place are still scarce. Two examples from the recent literature shall be discussed here. The first is the photochemical oxidation of organic substrates such as alcohols, ethers, or amides in the presence of water and α-$H_3PW_{12}O_{40}$ as a catalyst. The ^{183}W-NMR spectrum before and after dehydrogenation indicates that little if any decomposition of the catalyst occurs during the process[117]. The second example, the catalysis of the synthesis of substituted pyridines from alkynes and nitriles by organo-cobald compounds, is a more detailed study of an apparent correlation between catalytic activity/selectivity and the electron structure of the compound considered the catalyst or the precursor of an actually catalytically active inter-

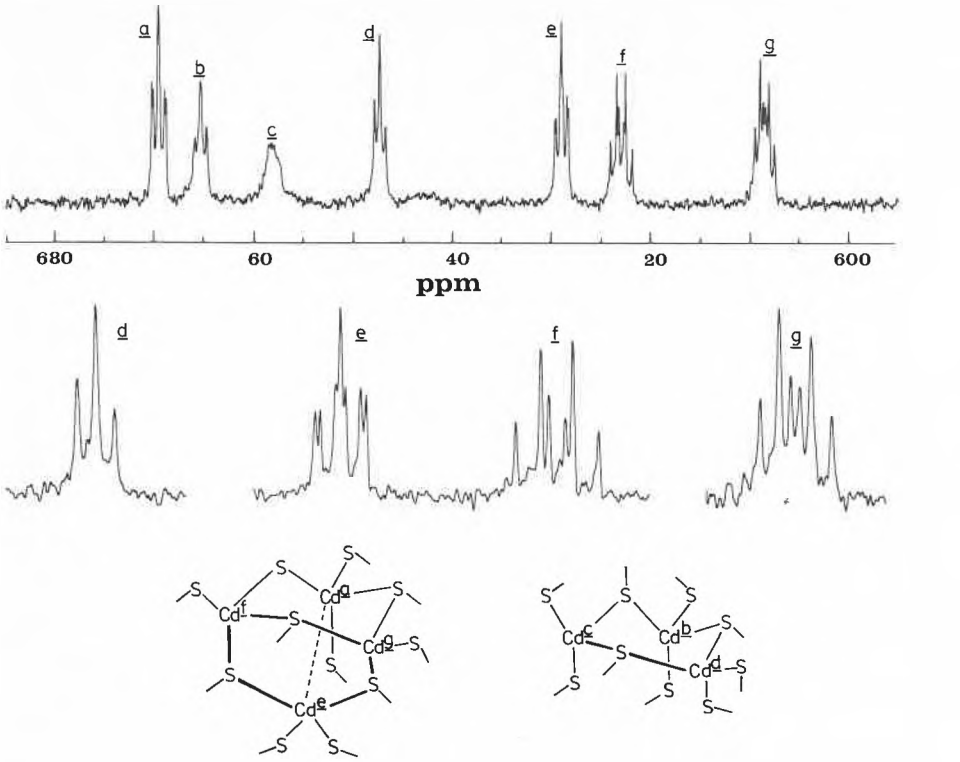

Fig. 19. $^{113}Cd\{^1H\}$-NMR spectrum of Cd_7-thionein (with the expansion of the signals d to g after resolution enhancement) and schematic representation of the two metal clusters. The letter beside each Cd refers to the corresponding resonance in the spectrum. ^{113}Cd-^{113}Cd two-bond scalar couplings take place along the Cd-S-Cd connectivities. The dashed line indicates four-bond coupling. The sulfur atoms are cystein residuals which built up ca. one third of the amino acid constitution of the protein. The shift scale is relative to 0.1 M aqueous $Cd(ClO_4)_2$[116].

mediate[118]. The key reaction is

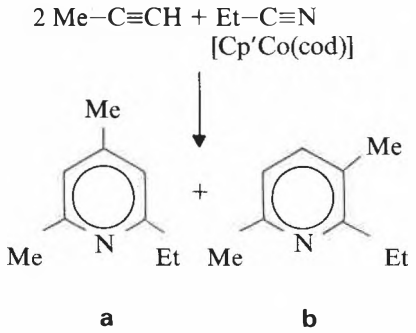

«cod» is 1,5-cyclooctadiene and Cp' substituted η^5-C_5H_5. The cod ligand dissociates off the metal under comparatively mild conditions; the active species therefore is thought to be the {Cp'Co} moiety. For this reaction, a correlation has been found between $\delta(^{59}Co)$ of the catalyst and both its catalytic activity and regioselectivity: The activity increases and the unsymmetrical isomer **(b)** is preferentially formed, as the shielding of the ^{59}Co nucleus decreases with increasing electron withdrawing ability of the substituents on the cyclopentadienyl ring.

8. Future Prospects

Improving instrumentation and increasingly sophisticated detection techniques will enable coordination chemists to focus their interest on the NMR detection of low sensitivity (low γ) nuclei such as ^{57}Fe[83,119,123], ^{103}Rh[55,123], $^{107,109}Ag$[57,120], and ^{183}W[84] and on problems where the nucleus under investigation is present in low molar concentrations only such as in biosystems (^{113}Cd[6,116], ^{67}Zn[110–113]) and in catalysis (^{59}Co[118]).

The availability of wide-bore high-field instruments for large sample volumes, supplied with broad band r.f. equipment and pulse generators for variable pulse sequences will increase the amount of data on nuclei with low resonance frequencies (cf. Table 1) and thus provide the material necessary for comparative (methodological and theoretical) studies with the already available set of information on the more established nuclei ^{51}V[3,4], ^{95}Mo[5], ^{55}Mn[3], ^{59}Co[3,21,123], and ^{195}Pt[7]. The newly available high-field technique, which can handle line-widths up to ca. 30 kHz, may also advantageously be employed to tackle measuring problems sometimes encountered with quadrupolar nuclei in sites of low local symmetry or centred in large molecules. Alternatively, wide-line equipment, working with a field-sweep, is the method of choice for problems arising with quadrupolar nuclei, if it comes to excessive line widths, low receptivities (note that the relative receptivities at constant measuring frequency are one order of magnitude better than at constant field B_0; cf. Table 1), or the detection of quadrupole interaction in (partially) anisotropic systems (^{93}Nb[97]; Fig. 17). The use of high-field instrumentation is not always an advantage: Quadrupole interactions, e.g., are suppressed; and for spin-½ nuclei, resolution may be deteriorated by an increase of line widths due to chemical shift anisotropy relaxation.

Innovation of detection methods[123] encompasses steady state techniques for nuclei resonating at extreme low field (^{103}Rh), polarization transfer (INEPT, DEPT) in complexes with coupling interactions between the metal and a ligand nucleus such as ^1H, ^{13}C, ^{15}N, or ^{31}P (e.g. in complexes of $^{107,109}Ag$[57,120], see **11** in Fig. 11), homonuclear (^{183}W-^{183}W[84], Fig. 16; ^{113}Cd-^{113}Cd[116]) and heteronuclear 2-dimensional methods (^{183}W-^{51}V in vanadotungstates[51]).

We have excluded, in this article, the rapidly developing NMR investigation of transition metal nuclei in solids, where dipole-dipole interaction, chemical shift anisotropy, and second order quadrupole perturbation cause additional problems which can be dealt with, in terms of resolution enhancement, by magic-angle and variable-angle sample spinning. The readar interested in this field should consult the pioneering work by *Oldfield* et al.[121] and, for current information, the Specialist Periodical Reports (RSC) on Nuclear Magnetic Resonance, edited by *G.A. Webb*.

Received: May 13, 1986 [FR 27]

[1] J.J. Dechter, *Prog. Inorg. Chem. 33* (1985) 393.
[2] a) R.K. Harris, E.E. Mann (Ed.): *NMR and the Periodic Table*, Academic Press, New York (1978); b) J. Mason (Ed.): *Multinuclear NMR*. Plenum, London, to be published (1986).
[3] D. Rehder, *Magn. Reson. Rev. 9* (1984) 125.
[4] D. Rehder, *Bull. Magn. Reson. 4* (1982) 33.
[5] M. Minelli, J.H. Enemark, R.T.C. Brownlee, M.J. O'Connor, A.G. Wedd, *Coord. Chem. Rev. 68* (1985) 169.
[6] P.D. Ellis, *Science 221* (1983) 1141.
[7] P.S. Pregosin, *Coord. Chem. Rev. 44* (1982) 247.
[8] A. Müller, E. Krickemeyer, H. Bögge, M. Penk, D. Rehder, *Chimia 40* (1986) 50.
[9] D. Rehder, W. Basler, *J. Magn. Reson.* (1986), in press.
[10] M. Hoch, D. Rehder, *J. Organomet. Chem. 288* (1985) C25; N.J. Coville, G.W. Harris, D. Rehder, *ibid. 293* (1985) 365.
[11] R. Talay, D. Rehder, *Inorg. Chim. Acta 77* (1983) L175.
[12] J. Schiemann, E. Weiss, *J. Organomet. Chem. 255* (1983) 175.
[13] F. Näumann, D. Rehder, *Z. Naturforsch. B39* (1984) 1647, 1654.
[14] F. Preuss, H. Becker, *Z. Naturforsch. B41* (1986) 185.
[15] J. Hanich, W. Willing, U. Müller, K. Dehnicke, D. Rehder, *Z. Naturforsch. B40* (1985) 1457; R. Christophersen, P. Klingelhöfer, U. Müller, K. Dehnicke, D. Rehder, *ibid. B40* (1985) 1631.
[16] B.N. Lamphun, G.A. Webb, *J. Mol. Struct. 104* (1983) 191.
[17] K. Kanda, H. Nakatsuji, Y. Yonezawa, *J. Am. Chem. Soc. 106* (1984) 5888.
[18] P.G. Gassman, W.H. Campbell, D.W. Macomber, *Organometallics 3* (1984) 385.
[19] G.M. Gray, C.S. Kraihanzel, *Inorg. Chem. 22* (1983) 2959.
[20] W. Priebsch, D. Rehder, *Inorg. Chem. 24* (1985) 3058.
[21] R.C. Kidd, *Annu. Rep. NMR Spectrosc. 10A* (1978) 1.

[22] S.F. Gheller, T.W. Hambley, J.R. Rodgers, R.T.C. Brownlee, M.J. O'Connor, R.M. Snow, A.G. Wedd, *Inorg. Chem. 23* (1984) 2519.
[23] N. Juranic, *Inorg. Chem. 22* (1983) 521.
[24] R. Bramley, M. Brorson, A.M. Sargeson, C.E. Schäffer, *J. Am. Chem. Soc. 107* (1985) 2780.
[25] N. Juranic, *Inorg. Chem. 24* (1985) 1599.
[26] K. Ihmels, D. Rehder, *Organometallics 4* (1985) 1334, 1340.
[27] R.T.C. Brownlee, A.F. Masters, M.J. O'Connor, A.G. Wedd, H.A. Kimlin, J.D. Cotton, *Org. Magn. Reson. 20* (1982) 73.
[28] G.M. Gray, R.J. Gray, D.C. Berndt, *J. Magn. Reson. 57* (1984) 347.
[29] A.F. Masters, R.T.C. Brownlee, M.J. O'Connor, A.G. Wedd, *Inorg. Chem. 20* (1981) 4283.
[30] M. Hoch, A. Duch, D. Rehder, *Inorg. Chem. 25* (1986), in press.
[31] D. Rehder, *J. Magn. Reson. 38* (1980) 419.
[32] G.T. Andrews, I.J. Colquhoun, W. McFarlane, S.O. Grim, *J. Chem. Soc. Dalton Trans.* (1982) 2353; *Polyhedron 2* (1983) 783.
[33] S. Heitkamp, D.J. Stufkens, K. Vrieze, *J. Organomet. Chem. 169* (1979) 107.
[34] M. Minelli, T.W. Rockway, J.H. Enemark, H. Brunner, M. Muschiol, P. Beier, *J. Organomet. Chem. 217* (1981) C34; *221* (1981) C40; H. Brunner, P. Beier, E. Frauendorfer, M. Muschiol, D.K. Rastogi, J. Wachter, M. Minelli, J.H. Enemark, *Inorg. Chim. Acta 96* (1985) L5.
[35] G.B. Benedek, R. Engleman, J.A. Armstrong, *J. Chem. Phys. 39* (1963) 3349.
[36] J.G. Russel, R.G. Bryant, *Anal. Chim. Acta 151* (1983) 227.
[37] P.C. Lauterbur, *J. Chem. Phys. 42* (1965) 799.
[38] V.P. Tarasov, V.I. Privalov, Yu.A. Buslaev, *Z. Naturforsch. B39* (1984) 1230.
[39] M. Hoch, D. Rehder, *Inorg. Chim. Acta 111* (1986) L13.
[40] M. Hoch, D. Rehder, unpublished results.
[41] C.J. Jameson, H.J. Osten. *Annu. Rep. NMR Spectrosc. 17* (1986), in press.
[42] G.E. Maciel, L. Simeral, J.J.H. Ackerman, *J. Phys. Chem. 81* (1977) 263.
[43] B.W. Epperlein, H. Krüger, O. Lutz, A. Schwenk, *Z. Naturforsch. B40* (1985) 363.
[44] G. Navon, W. Kläui, *Inorg. Chem. 23* (1984) 2722.
[45] F. Preuss, E. Fuchslocher, W.S. Sheldrick, *Z. Naturforsch. B40* (1985) 363.
[46] O.W. Howarth, M. Jarrold, *J. Chem. Soc. Dalton Trans.* (1978) 503.
[47] R.I. Maksimovskaya, K.G. Burtseva, *Polyhedron 4* (1985) 1559.
[48] M.J. Gressner, A.S. Tracey, *J. Am. Chem. Soc. 107* (1985) 4215.
[49] M.T. Pope: *Heteropoly and Isopoly Oxometalates*, Inorganic Chemistry Concepts, Vol. *8*, Springer-Verlag, Berlin (1983).
[50] C. Brevard, R. Schimpf, G. Tourne, C.M. Tourne, *J. Am. Chem. Soc. 105* (1983) 7059.
[51] P.J. Domaille, *J. Am. Chem. Soc. 106* (1984) 7677; P.J. Domaille, W.H. Knoth, *Inorg. Chem. 22* (1983) 818.
[52] S.F. Gheller, T.W. Hambley, R.T.C. Brownlee, M.J. O'Connor, M.R. Snow, A.G. Wedd, *J. Am. Chem. Soc. 105* (1983) 1527.
[53] W.A. Herrmann, H. Biersack, M.L. Ziegler, K. Weidenhammer, R. Siegel, D. Rehder, *J. Am. Chem. Soc. 103* (1981) 1692.
[54] T. Saito, S. Sawada, *Bull. Chem. Soc. Jpn. 58* (1985) 459.
[55] B.T. Heaton, L. Strona, R.D. Pergola, L. Garlaschelli, U. Satorelli, I.H. Sadler, *J. Chem. Soc. Dalton Trans.* (1983) 173.
[56] G. Doyle, B.T. Heaton, E. Occhiello, *Organometallics 4* (1985) 1224.
[57] S.S.D. Brown, I.J. Colquhoun, W. McFarlane, M. Murray, I.D. Salter, V. Sik, *J. Chem. Soc. Chem. Commun.* (1986) 53.
[58] S.J. Anderson, P.L. Goggin, R.J. Goodfellow, *J. Chem. Soc. Dalton Trans.* (1976) 1959.
[59] V.P. Tarasov, T.Sh. Kapanadze, V.S. Tsintsadze, Yu.A. Buslaev, *Koord. Khim. 9* (1983) 647.
[60] E.C. Alyea, G. Ferguson, A. Somogyvari, *Organometallics 2* (1983) 668.
[61] P. Bougard, M. Mancini, B.G. Sayer, M.J. McGlinchey, *Inorg. Chem. 24* (1985) 93.
[62] J. Grobe, J. Vetter, D. Rehder, *Z. Naturforsch. B40* (1985) 975.
[63] E. Haid, D. Köhnlein, G. Kössler, O. Lutz, W. Messner, K.R. Mohn, G. Nothaft, B. van Rickelen, W. Schich, N. Steinhauser, *Z. Naturforsch. A38* (1983) 317.
[64] A.M. Bond, R. Colton, J.E. Moir, D.R. Page, *Inorg. Chem. 24* (1985) 1298.
[65] V.P. Tarasov, V.I. Privalov, Yu.A. Buslaev, *Mol. Phys. 35* (1978) 1047.
[66] P.S. Pregosin, M. Kretschmer, W. Preetz, G. Rimkus, *Z. Naturforsch. B37* (1982) 1422.
[67] K. Endo, K. Yamamoto, K. Matsushita, K. Deguchi, *J. Magn. Reson. 65* (1985) 268.
[68] R. Benn, A. Rufinska, *J. Organomet. Chem. 273* (1984) C51.
[69] G.F.P. Warnock, S.B. Philson, J.E. Ellis, *J. Chem. Soc. Chem. Commun.* (1984) 893.
[70] M. Minelli, J.L. Hubbard, K.A. Christensen, J.H. Enemark, *Inorg. Chem. 22* (1983) 2652.
[71] C.J. Besecker, W.G. Klemperer, D.J. Maltbie, D.A. Wright, *Inorg. Chem. 24* (1985) 1027.
[72] K.H.A. Ostoja Starzewski, P.S. Pregosin, *Angew. Chem. 92* (1980) 323; *Angew. Chem. Int. Ed. Engl. 19* (1980) 316.
[73] M. Kretschmer, P.S. Pregosin, P. Farve, C.W. Schlaepfer, *J. Organomet. Chem. 253* (1983) 17.
[74] A. Albinati, C.G. Anklin, P.S. Pregosin, *Inorg. Chim. Acta 90* (1984) L37; C.G. Anklin, P.S. Pregosin, *Magn. Reson. Chem. 23* (1985) 671.
[75] D. Rehder, H.-C. Bechthold, A. Kececi, H. Schmidt, M. Siewing, *Z. Naturforsch. B37* (1982) 631.
[76] D.S. Milbrath, J.G. Verkade, R.J. Clark, *Inorg. Nucl. Chem. Lett. 12* (1976) 921.
[77] R.M. Nielson, S. Wherland, *Inorg. Chem. 23* (1984) 3265.
[78] Y. Kawada, T. Sugawara, H. Iwamura, *J. Chem. Soc. Chem. Commun.* (1979) 291.
[79] T.H. Köhler, H.J. Kalder, E.O. Fischer, *J. Organomet. Chem. 113* (1976) 11.
[80] S.O. Grim, D.P. Shah, *Inorg. Nucl. Chem. Lett. 14* (1978) 105.
[81] B.G. Sayer, J.I.A. Thompson, N. Hao, T. Birchall, D.R. Eaton, M.J. McGlinchey, *Inorg. Chem. 20* (1981) 3748.
[82] J.K. Beattie, *Inorg. Chem. 10* (1971) 426; J.K. Beattie, L.H. Novak, *J. Am. Chem. Soc. 93* (1971) 620.
[83] a) A.A. Koridze, N.M. Astakhova, P.V. Petrovskii, *J. Organomet. Chem. 254* (1983) 345; b) W.J. Evans, J.H. Maedows, T.P. Hanusa, *J. Am. Chem. Soc. 106* (1984) 4454; c) W.J. Evans, J.H. Meadows, A.G. Kostka, G.L. Closs, *Organometallics 4* (1985) 324.
[84] W.H. Knoth, P.J. Domaille, D.C. Roe, *Inorg. Chem. 22* (1983) 198.
[85] R.J. Gillespie, P. Granger, K.R. Morgan, G.J. Schrobilgen, *Inorg. Chem. 23* (1984) 887.
[86] G.F.P. Warnock, J.E. Ellis, *J. Am. Chem. Soc. 106* (1984) 5016.
[87] Yu. A. Buslaev, G.A. Kirakosian, V.P. Tarasov, *Dokl. Akad. Nauk. SSSR 264* (1982) 1450.
[88] S.C.F. Au-Yeung, R.J. Buist, D.R. Eaton, *J. Magn. Reson. 55* (1983) 24; S.C.F. Au-Yeung, D.R. Eaton, *ibid. 52* (1983) 351, 366.
[89] J.J. Dechter, J. Kowalewski, *J. Magn. Reson. 59* (1984) 146.
[90] O. Groning, T. Drakenberg, L.I. Elding, *Inorg. Chem. 21* (1982) 1820.
[91] H.C. Lee, J.K. Gard, T.L. Brown, E. Oldfield, *J. Am. Chem. Soc. 107* (1985) 4087.
[92] L. Baltzer, E.D. Becker, R.G. Tschudin, O.A. Gansow, *J. Chem. Soc. Chem. Commun.* (1985) 1040.
[93] D. Köhnlein, O. Lutz, P. Ruppert, *J. Magn. Reson. 57* (1984) 486.
[94] R.T.C. Brownlee, M.J. O'Connor, B.P. Shenan, A.G. Wedd, *J. Magn. Reson. 61* (1985) 516.
[95] K. Paulsen, D. Rehder, *Z. Naturforsch. A37* (1982) 139.
[96] A.S. Tracey, K. Radley, *Can. J. Chem. 63* (1985) 2181.
[97] D. Rehder, K. Paulsen, W. Basler, *J. Magn. Reson. 53* (1983) 500.
[98] S. Bristow, C.D. Garner, S.K. Hagyard, G.A. Morris, J.R. Nicholson, C.F. Mills, *J. Chem. Soc. Chem. Commun.* (1985) 479.
[99] B. Borah, C.W. Chen, W. Egan, M. Miller, A. Wlodawer, J.S. Cohen, *Biochemistry 24* (1985) 2058.
[100] G.M. Clove, A.M. Gronenborn, *J. Am. Chem. Soc. 104* (1982) 1369.
[101] M. Minelli, C.G. Young, J.H. Enemark, *Inorg. Chem. 24* (1985) 1111.
[102] M. Minelli, J.H. Enemark, K. Wieghardt, M. Hahn, *Inorg. Chem. 22* (1983) 3952.
[103] K.A. Christensen, P.E. Miller, M. Minelli, T.W. Rockway, J.H. Enemark, *Inorg. Chim. Acta 56* (1981) L27.
[104] E.C. Alyea, J. Topich, *Inorg. Chim. Acta 65* (1982) L95.
[105] S.F. Gheller, T.V. Hambley, P.R. Traill, R.T.C. Brownlee, M.J. O'Connor, M.R. Snow, A.G. Wedd, *Aust. J. Chem. 35* (1982) 2183.
[106] M. Minelli, K. Yamanouchi, J.H. Enemark, P. Subramanian, B.P. Kaul, J.T. Spence, *Inorg. Chem. 23* (1984) 2554.
[107] S.F. Gheller, T.W. Hambley, J.R. Rodgers, R.T.C. Brownlee, M.J. O'Connor, M.A. Snow, A.G. Wedd, *Inorg. Chem. 23* (1984) 2519.
[108] M. Minelli, J.H. Enemark, J.R. Nicholson, C.D. Garner, *Inorg. Chem. 23* (1984) 4384.
[109] B.M. Hoffman, J.E. Roberts, W.H. Orme-Johnson, *J. Am. Chem. Soc. 104* (1982) 860.
[110] T. Shimizu, M. Hatano, *Biochem. Biophys. Res. Commun. 104* (1982) 1356.
[111] T. Shimizu, M. Hatano, *Biochem. Biophys. Res. Commun. 115* (1983) 22.
[112] T. Shimizu, M. Hatano, *Inorg. Chem. 24* (1985) 2003.
[113] T. Shimizu, M. Hatano, *Inorg. Chim. Acta 76* (1983) L177.
[114] T. Nozawa, M. Sato, M. Hatano, N. Kobayashi, T. Osa, *Chem. Lett.* (1983) 1289.
[115] J.D. Otvos, I.M. Armitage, *Proc. Natl. Acad. Sci. USA 77* (1980) 7094.
[116] J.D. Otvos, H.R. Engeseth, S. Wehrli, *Biochemistry 24* (1985) 6735.
[117] C.L. Hill, D.A. Bouchard, *J. Am. Chem. Soc. 107* (1985) 5148.
[118] H. Bönnemann, W. Brijoux, R. Brinkmann, W. Meurers, R. Mynott, W. von Phillipsborn, T. Egolf, *J. Organomet. Chem. 272* (1984) 231; H. Bönnemann, *Angew. Chem. 97* (1985) 264; *Angew. Chem. Int. Ed. Engl. 24* (1985) 248.
[119] T. Jenny, W. von Philipsborn, J. Kronenbitter, A. Schwenk, *J. Organomet. Chem. 205* (1981) 211.
[120] G.C. van Stein, G. van Koten, K. Vrieze, C. Brevard, A.L. Spek, *J. Am. Chem. Soc. 106* (1984) 4486.
[121] E. Oldfield, R.A. Kinsey, B. Montez, T. Ray, K.A. Smith, *J. Chem. Soc. Chem. Commun.* (1982) 254; S. Ganapathy, S. Schramm, E. Oldfield, *J. Chem. Phys. 77* (1982) 4360.
[122] L. Baltzer, E.D. Becker, B.A. Averill, J.M. Hutchinson, O.A. Gansow, *J. Am. Chem. Soc. 106* (1984) 2444.
[123] W. von Philipsborn, *Pure Appl. Chem. 58* (1986) 513.